Naval Surface Warfare Center

Carderock Division

West Bethesda, MD 20817-5700

NSWCCD-80-TR-2016/033 **November 2016**

Naval Architecture and Engineering Department

Technical Report

A CONSISTENT WAVE IMPACT LOAD MODEL FOR STUDYING STRUCTURE, EQUIPMENT RUGGEDNESS, SHOCK ISOLATION SEATS, AND HUMAN COMFORT IN SMALL HIGH-SPEED CRAFT

by

Michael R. Riley, The Columbia Group
Heidi P. Murphy, NSWCCD
Dr. Timothy W. Coats, NSWCCD

THIS PAGE INTENTIONALLY LEFT BLANK

REPORT DOCUMENTATION PAGE

Form Approved
OMB No. 0704-0188

1. REPORT DATE	**2. REPORT TYPE**	**3. DATES COVERED** *(From - To)*
30-11-2016	Final	Sep 2015 to Oct 2016

4. TITLE AND SUBTITLE
A Consistent Wave Impact Load Model for Studying Structure, Equipment Ruggedness, Shock Isolation Seats, and Human Comfort in Small High-Speed Craft

5a. CONTRACT NUMBER

5b. GRANT NUMBER

5c. PROGRAM ELEMENT NUMBER

6. AUTHOR(S)
Michael R. Riley (TCG), Heidi P. Murphy , Dr. Timothy W. Coats

5d. PROJECT NUMBER

5e. TASK NUMBER

5f. WORK UNIT NUMBER

7. PERFORMING ORGANIZATION NAME(S) AND ADDRESS(ES)
NAVSEA Carderock
Naval Surface Warfare Center
Carderock Division (Code 83)
9500 Macarthur Boulevard
West Bethesda, MD 20817-5700

8. PERFORMING ORGANIZATION REPORT NUMBER
NSWCCD-80-TR-2016/033

9. SPONSORING / MONITORING AGENCY NAME(S) AND ADDRESS(ES)
NAVSEA Carderock
Naval Surface Warfare Center
Carderock Division
9500 MacArthur Blvd
West Bethesda, MD 20817-5700

10. SPONSOR/MONITOR'S ACRONYM(S)

11. SPONSOR/MONITOR'S REPORT NUMBER(S)

12. DISTRIBUTION / AVAILABILITY STATEMENT
DISTRIBUTION STATEMENT A. Approved for public release; distribution is unlimited.

13. SUPPLEMENTARY NOTES

14. ABSTRACT
This report presents a new integrated approach to investigating the effects of wave impacts on hull structure, equipment ruggedness, shock isolation seats, and human comfort in small high-speed planing craft. Acceleration data recorded during full-scale seakeeping trials are presented to illustrate lessons learned from deterministic studies of individual wave impacts, and use of a consistent wave impact load model is presented. Implications for further research are also presented.

15. SUBJECT TERMS
Wave impact planing craft acceleration data analysis

16. SECURITY CLASSIFICATION OF:			**17. LIMITATION OF ABSTRACT**	**18. NUMBER OF PAGES**	**19a. NAME OF RESPONSIBLE PERSON**
					Dr. Timothy Coats
a. REPORT	**b. ABSTRACT**	**c. THIS PAGE**			**19b. TELEPHONE NUMBER**
Unclassified	Unclassified	Unclassified	See 12.	64	757-462-4161

Standard Form 298 (Rev. 8-98)
Prescribed by ANSI Std. Z39.18

THIS PAGE INTENTIONALLY LEFT BLANK

CONTENTS

FIGURES

TABLES

THIS PAGE INTENTIONALLY LEFT BLANK

SYMBOLS, ABBREVIATIONS, AND ACRONYMS

π ..... ratio of circle circumference to its diameter

$\overline{A}$ ..... average acceleration

$A_{1/N}$ ..... average of highest $1/N^{th}$ peak accelerations

A_{MAX} ..... maximum or peak acceleration

a_W ..... frequency weighted (i.e., band-pass filtered) acceleration

A(t) ..... acceleration time history

ASRS ..... acceleration shock response spectrum

c ..... damping coefficient

deg ..... degrees

DSRS ..... relative displacement shock response spectrum

g ..... acceleration due to gravity (32.2 ft/sec^2, 9.81 m/sec^2)

Hz ..... Hertz (cycles per second)

$H_{1/N}$ ..... average of highest $1/N^{th}$ wave heights

L ..... craft length

lbs ..... pounds

LCG ..... longitudinal center of gravity

ISO ..... International Standards Organization

LCG ..... longitudinal center of gravity

k ..... stiffness

K ..... kilo (e.g. 1000)

m ..... mass

m or msec ..... millisecond

MR ..... mitigation ratio

PVSRS ..... pseudo-velocity shock response spectrum

RMQ ..... root mean quad

RMS ..... root mean square

R ..... ratio of shock pulse duration to natural frequency

SDOF ..... single degree of freedom

SRS .....shock response spectrum
t ..... time
T..... wave impact shock pulse duration
V or V_S.....craft average speed
VDV..... vibration dose value
x ..... surge axis positive forward
y .....sway axis positive to port
z.....surge axis positive up
%.....percent
Δ ..... maximum relative displacement
ϖ ..... circular frequency

ADMINISTRATIVE INFORMATION

This report was prepared by the Combatant Craft Division (CCD, Code 83) of the Naval Architecture and Engineering Department at the Naval Surface Warfare Center, Carderock Division (NSWCCD) with funding provided by Naval Surface Warfare Center, Carderock Division under the Naval Innovative Science and Engineering (NISE) Section 219 research and development program.

ACKNOWLEDGEMENTS

The authors would like to thank Dr. Jack L. Price, Director of Research, Naval Surface Warfare Center, Carderock Division for overall management of wave slam phenomenology and craft motion mechanics investigations. During different periods of the investigations numerous individuals contributed significant information based on their naval architecture and marine engineering experiences related to high-speed craft. From Naval Sea Systems Command this included Malcolm (Mack) Whitford and Dean Schleicher, and from the Combatant Craft Division of NSWCCD it included Willard Sokol, Carl Casamassina, Jason Marshall, Donald Jacobson, Richard Wilson, Scott Petersen, Larry Michelon, Alma Jacobson, David Pogorzelski, Kelly Haupt, Neil Ganey, Jayson Bautista, Brock Aron, and Tom Kush. Their expertise in combatant craft design and acquisition, systems integration, and seakeeping trials data acquisition and their willingness to share is sincerely appreciated.

THIS PAGE INTENTIONALLY LEFT BLANK

Summary

This report presents a new integrated approach to investigating the effects of wave impacts on hull structure, equipment ruggedness, shock isolation seats, and human comfort in small high-speed planing craft. Acceleration data recorded during full-scale seakeeping trials are presented to illustrate lessons learned from recent studies of individual wave impacts. Example applications are presented to show how use of both statistical and deterministic methodologies address a broader range of design and comparative analysis topics than obtained from a single approach. Implications for further research are also presented.

Introduction

For craft that operate beyond calm sea conditions the study of seakeeping is synonymous with the study of wave effects on dynamic stability, structural integrity, effects on equipment, and effects on human comfort, safety, and performance, *Blount (2014)*. The earliest studies of high-speed craft in waves faced major challenges, especially in the field of instrumentation and data acquisition. Even with advances in electronics it was extremely challenging because of limited data processing methods for interpreting the recorded motions. The subsequent introduction of computer hardware and data processing software fostered the development of statistical approaches for hull design and methods for assessing wave impact effects on humans.

The following paragraphs provide a broad overview of early data acquisition and numerous statistical approaches that evolved for studying hull strength and human ride quality. The review illustrates the importance of their evolutionary development with advances in data processing capacity. But there is sufficient justification now to also pursue a new non-statistical approach. This is especially true in light of advanced data analysis software not widely available 15 years ago.

Hull Structure Impact Load

The earliest hull design studies focused on underwater pressure, acceleration, and strain data to study wave impact loads during seakeeping trials. Figure 1 shows pressure data and acceleration data recorded during high-speed craft trials of a naval support craft in the mid-1940's. Figure 2 shows pressure, hull strain, and acceleration data recorded in the 1950's, *DuCane (1956)*. Peak amplitudes were determined manually using adjustable scales (e.g., Gerber Variable Scale ^{TM}) and values were hand printed on paper plots referred to as strip charts.

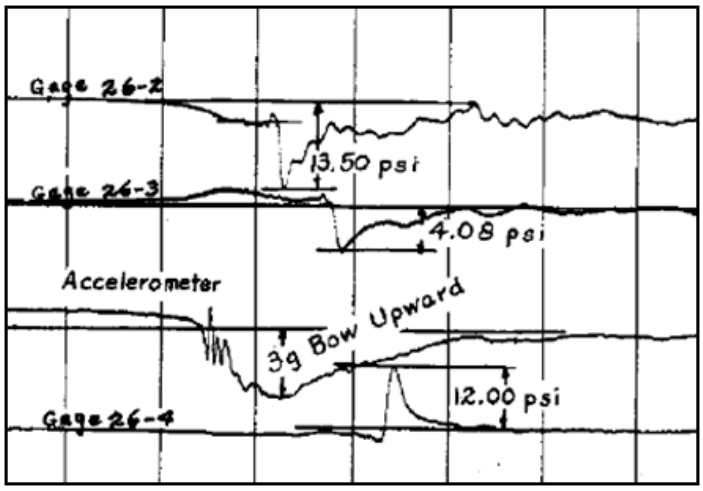

Figure 1. Example Craft Data Circa 1944.

Figure 2. Craft Data Circa 1956

In rough seas the relationship between the wave impact pressure distribution and the dynamic response of the craft is very complex. Simplifying assumptions were therefore made that assumed the net vertical force at a hull cross-section due to the pressure distribution at any instant in time is directly proportional to the heave acceleration response at that cross-section, *Heller and Jasper (1960)*. The heave acceleration at a cross-section was used as a measure of the wave impact load in units of g. Later developments included publication of the envelope of the maximum vertical acceleration (or impact load factor) for varying craft displacement as shown in Figure 3. The impact load factor was used to compute an effective static design pressure, *Allen and Jones (1978).*

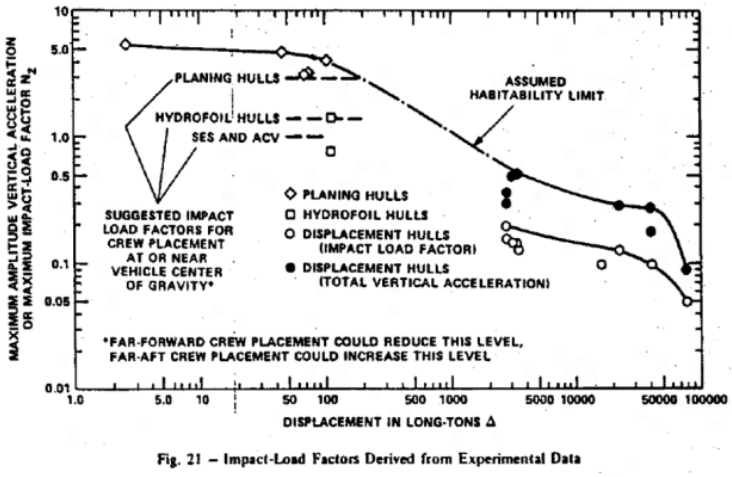

Figure 3. Maximum Vertical Acceleration

The paper by *Allen and Jones (1978)* acknowledged that the most difficult and controversial step in the hull design pressure calculation was selection of the impact load factor. For planing hulls the paper referenced work by *Savitsky and Brown (1976)* whose significant contributions included an empirical equation for computing the average vertical acceleration (i.e., $A_{AVG,}$ the average of many impact peak accelerations) at the longitudinal center of gravity (LCG) as a function of wave height, speed, craft deadrise, beam, length, and weight. The empirical equation was based on scale-model data for irregular seas analyzed to determine its statistical distribution, *Fridsma (1971)*. The $A_{1/N}$ approach included scaling from the A_{AVG} acceleration using the following theoretical equations for the exponentially distributed scale-model data. The coefficients in each equation vary for different distribution models.

$$A_{1/N} = A_{AVG}\left[1+\ln\left(N\right)\right] \qquad \text{Equation (1)}$$

$$A_{1/3} = 2.1A_{AVG}$$

$$A_{1/10} = 3.3A_{AVG}$$

$$A_{1/100} = 5.6A_{AVG}$$

These statistics were referred to as averages of the highest $1/N^{th}$ peak accelerations from origins in earlier oceanographic studies where wave height distributions were described by averages of the highest $1/N^{th}$ wave heights, *Munk (1944)*. The same statistical approach was used to develop an empirical equation for $A_{1/10}$ based on analysis of full-scale seakeeping data, *Hoggard and Jones (1980)*. Ship classification societies continued the statistical paradigm by publishing equations for computing the $A_{1/100}$ parameter as an impact load factor used in equations for the effective pressure to be used in hull design analyses. Some naval architects, not all, argued that the $A_{1/10}$ statistic was more appropriate for hull design, *Koelbel (2001)*.

Ride Quality

The study of human comfort and performance at sea in high-speed craft was also an important topic during the early 1970's. Approaches to quantifying wave slam exposure were being investigated and shock isolation seats adapted from airplane landing struts and land vehicle designs were in development. Figure 4 shows acceleration data recorded on a Moulton suspension seat in a 31-foot craft operating in rough seas, *Ducane (1971)*. It shows from top to bottom the boat vertical acceleration, seat vertical acceleration, seat relative displacement, and seat relative velocity.

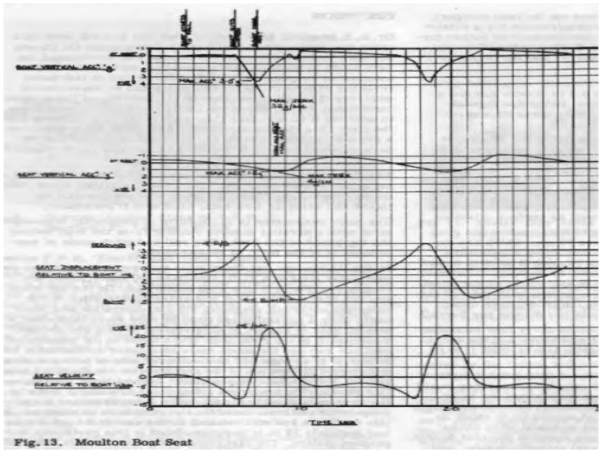

Figure 4. Shock Isolation Seat Response

Figure 5 shows an early design of an adjustable shock isolation seat, *Pickford, et al., (1975)* and acceleration data for two seats recorded on the deck and on the seat during patrol boat trials.

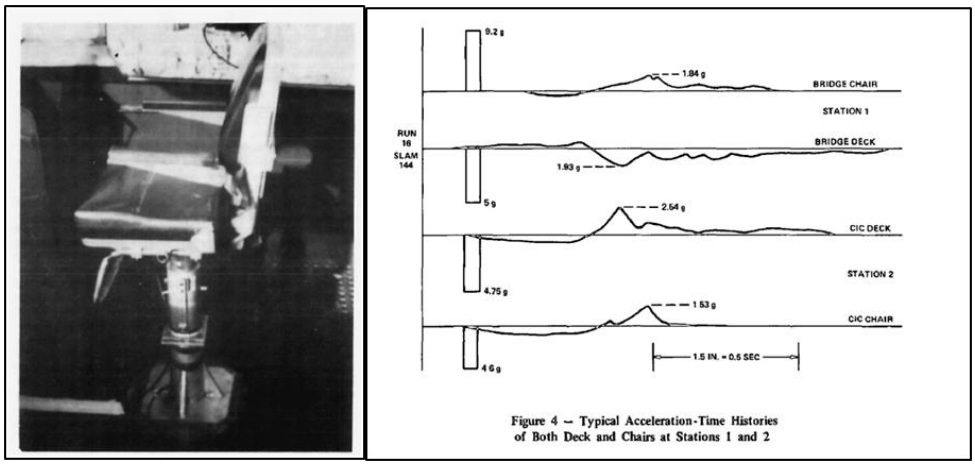

Figure 5. Naval Patrol Boat Shock Isolation Seat

The successful acquisition of motion data did not however lead to agreement on parameters for quantifying ride quality (or ride roughness) in the marine environment. There was a general dissatisfaction with the lack of valid hard data upon which meaningful comparisons between different craft could be based, and there was no fully satisfactory criterion for judging the ride quality of high-speed craft in rough seas, *Ellsworth* (1974). The introduction of new computer systems significantly improved signal processing and the computation of statistical parameters. Previous manual analysis of data strip charts was replaced with signal processing algorithms. Initially, lessons learned from airline and automobile vibration environment studies influenced marine vehicle researchers who applied the statistical root mean square (RMS) acceleration criteria to compare the motions experienced on displacement hulls, surface effects ships, and hydrofoils with established criteria for motion sickness and fatigue, *NASA (1972)* and *Stark (1980)*.

The RMS parameter was also used to establish criteria for fatigue-decreased proficiency, *ISO 2631-1 (1985)* and motion sickness. But the RMS value of vertical accelerations in a high-speed craft was known to be much less than the amplitude of the majority of peak accelerations caused by impacts. Other statistical parameters were therefore introduced with 4^{th}-order terms in an attempt to emphasize the larger peaks. For example, the root mean quad (RMQ) and the vibration dose value (VDV) were introduced, *Boileau, Turcot, and Scory (1989)*. The VDV is given by equation (1-5) where a_W (t) is the recorded acceleration signal after being subjected to a band-pass filter (i.e., frequency weighting) specified for seated or standing positions.

$$VDV = \left[\int_0^T a_w^4(t)\,dt \right]^{\frac{1}{4}} \qquad \text{Equation (1-5)}$$

The VDV is used for quantifying human exposure to whole body vibrations with intermittent shocks, *ISO-2631 - 1 (1997)*. There is also a 6^{th}-power statistical parameter for estimating adverse health effects on the spine of a seated human due to whole body vibrations containing multiple shocks, *ISO-2631-5 (2004)* and *Petersen, et al. (2004*).

Another statistical approach initially used by naval craft designers in the 1970's used vertical $A_{1/10}$ values at the LCG to characterize different levels of ride quality in terms of human comfort and performance, *Savitsky and Koelbel (1978)*. Table 1 was published much later to show the $A_{1/10}$ values and descriptions of crew effects in high-speed planing craft, *Savitsky and Koelbel* (1993). It was reported that acceleration levels for crew tolerance and structural design are most frequently given as the average of the one-tenth highest accelerations, but there was no intrinsic reason why this statistic should be used. "It probably came about because observers felt that this level best represented, with a single number, their experience of the actual random accelerations in much the same way that oceanographers characterize the random waves of a sea state by the average of the one-third highest*", Savitsky and Koelbel (1993).*

Table 1. 1993 Crew Comfort and Performance Criteria

$A_{1/10}$ (g) at LCG	Effects on Personnel
1.0	Maximum for millitary function long term (over 4 hours)
1.5	Maximum for military function short term (1 - 2 hours)
2.0	Tests discontinued
3.0	Extreme discomfort
4.0	
5.0	Physical injury
6.0	Military crew under fire

Observations

Interpretation of recorded accelerations like the data shown in Figures 1, 2, 4 and 5 focused on the effects of individual wave impacts, primarily because they were recorded before the introduction of computers and signal processing algorithms. As research continued, however, the literature shows that the study of hull structural strength and human comfort evolved with a reliance on statistical parameters to quantify the wave impact environment. This was a natural evolution dealing with wave height environments or irregular seas best characterized by statistical methods. The evolution of computer data processing in the early 1970's significantly reduced the arduous task of analyzing acceleration records that previously had to be read by hand, *Savitsky and Brown (1975)*. But the development of these methods across diverse communities of interest resulted in different statistical approaches for quantifying wave impact load for different applications. All the statistical methods relied on either full-scale or model-scale acceleration data, but there is no common engineering rationale nor was there consistency in the metrics for quantifying wave impact load. Some use the average of many peak accelerations, like $A_{1/N}$ values, while others use parameters that average entire signals over time after applying 2^{nd} order, 4^{th} order, or 6^{th} order exponents to each digitized point in a record.

Recent studies suggest that future advances in high-speed craft methodologies can benefit from an integrated approach that combines statistical information with a better understanding of the physics of individual wave impacts. Forty-five years ago the study of individual wave impacts could take hours, days, or weeks to analyze. Now the use of desktop computers with large gigabyte storage capacity and new general purpose data analysis software can do similar work in seconds, minutes, or hours. The following paragraphs summarize lessons learned from the recent study of individual wave impacts, referred to as wave impact determinism.

The Deterministic Approach

Craft Motion Mechanics

In 2005 a research project was initiated to understand why statistical acceleration values (e.g., $A_{1/N}$) documented in historical test reports from different agencies could not be used in craft comparative analyses, *Jacobson et al. (2007)*. Methods to extract peak accelerations were implemented subjectively by different analysts, which invariably led to processed peak accelerations that were not comparable. One of the products of this study was the standardized process for computing $A_{1/N}$ values referred to as StandardG[1], *Riley, Haupt, and Jacobson. (2010a)*. The research evolved further into a pursuit of a better understanding of craft motion mechanics and the cause-and-effect physical relationships between impact loading and craft responses. Figure 6 shows an unfiltered acceleration time history of three wave impacts. The responses to each impact damp out before the next wave impact. This simple impact and response relationship, observed even in the most flexible craft locations, provides the engineering justification for analyzing responses to wave impacts one at a time. The first step in analyzing (i.e., separation into its fundamental parts) acceleration data is to decompose the acceleration signal.

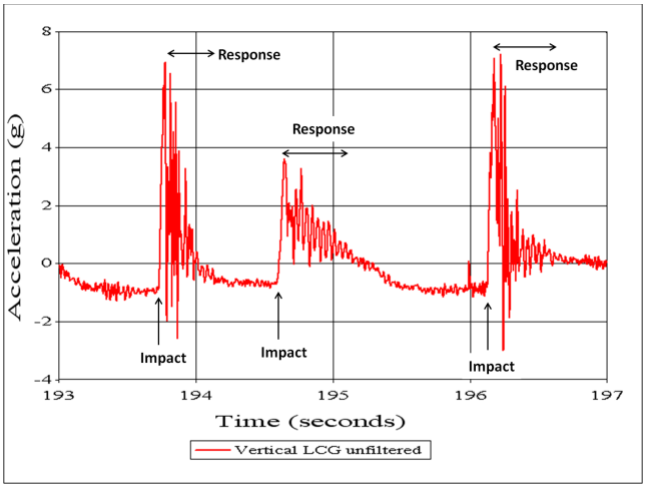

Figure 6. Wave Slam Input and Response Phenomena[2]

[1] Available free of charge by contacting the Branch Head of the United States Naval Academy Hydrodynamics Laboratory. Contact information is available at www.usna.edu/Hydrodynamics/Contact.php.
[2] All data plots shown in the report were created using UERDTools, Mantz and *Costanzo (2009)*.

Response Mode Decomposition

Accelerometers are very sensitive instruments that measure relative and absolute (i.e., rigid body) motions simultaneously. In marine craft the relative motions include millimeter deck vibrations caused by propulsion systems, power generation machinery, and forced structural vibrations during and after a wave impact. The absolute motions include heave, surge, and sway. The heave acceleration is an important measure relevant to the study of shock (i.e., wave slam) load transmission within a craft structure, *Riley, Coats, and Murphy (2014a).* Rigid body acceleration in surge and sway can also be important, but the vertical heave acceleration is typically the largest. The analysis of wave slam shock effects therefore requires that raw acceleration data be low-pass filtered to attenuate the vibration content in the record, leaving the majority content in the filtered record attributed to rigid body content. Figure 7 illustrates the response mode decomposition process of separating rigid body and vibration accelerations. The plot on the left shows a time history of the raw vertical acceleration (gray line) and the rigid body heave acceleration (dark black line) obtained by low-pass filtering. The rigid body heave acceleration is typically that motion about which the local vibrations oscillate. The plot on the right shows the vibration content obtained by high-pass filtering the recorded acceleration. The use of response mode decomposition to remove the seemingly random vibration signals recorded at different locations in different craft led to observations of rigid body motions during wave impacts that provide the foundation for pursuing a new deterministic approach to the study of wave slam phenomena.

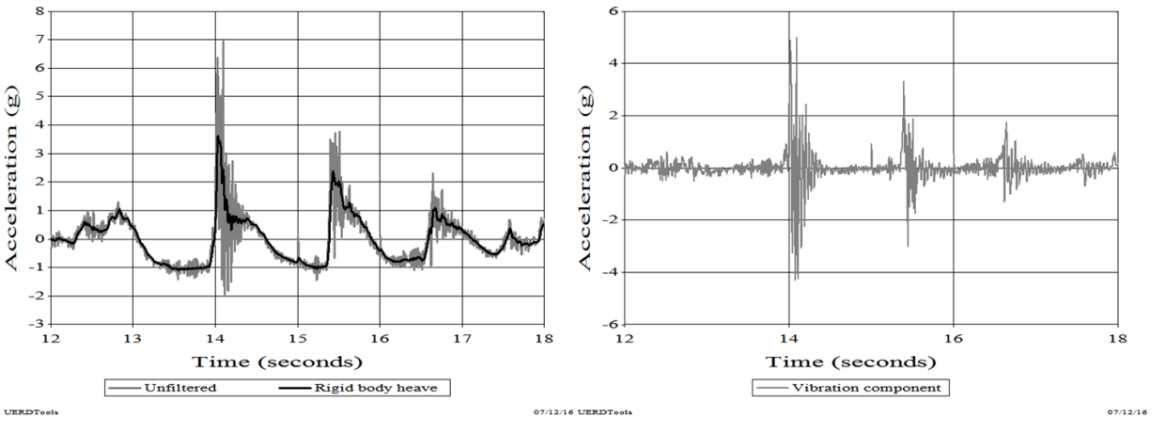

Figure 7. Rigid Body and Vibration Accelerations

Appendix A presents guidance on data filtering and selection of a low-pass filter for estimating rigid body acceleration.

Individual Wave Slam Observations

The Combatant Craft Division of Naval Surface Warfare Center Carderock Division has conducted full-scale seakeeping trials of many craft since its establishment in 1967. Consistent testing protocols provide a useful data base for observing interesting trends. The lessons learned summarized herein were based on analysis results for craft that weighed approximately 14,000 pounds (6.35 metric tons) to 116,000 pounds (52.6 metric tons) with lengths that varied from 33 feet (10 meters) to 82 feet (25 meters). Deadrise values varied from 18 to 22 degrees, *Riley, Coats, and Murphy (2014b).*

Sequence of Events

A vertical acceleration time history for one wave impact sequence and the velocity and absolute displacement (i.e., heave) curves obtained by integration are shown left to right in Figure 8. The curves illustrate the wave impact period and non-impact periods. At time A, the -0.9 g vertical acceleration indicates a condition very close to free fall. The relatively constant -0.9 g from time A to time B and the linear decrease in velocity suggests that the craft is rotating downward with the stern in the water. The drop in height from time A to B is most likely a combination of heave and pitch. At time B, the craft impacts the incident wave, the velocity is at a minimum, the negative slope changes rapidly to a positive slope, and the force of the wave impact produces a sharp rise in acceleration. From time B to time C, the craft continues to move down in the water, the velocity approaches zero, and the acceleration decreases rapidly. At time C the downward displacement of the craft reaches a maximum, the instantaneous velocity is zero, and the impact event is complete. From time C to D forces due to buoyancy, hydrodynamic lift, and components of thrust and drag combine to produce a net positive acceleration. From time D to E, gravity overcomes the combined forces of buoyancy, hydrodynamic lift, and components of thrust and drag as another wave encounter sequence begins.

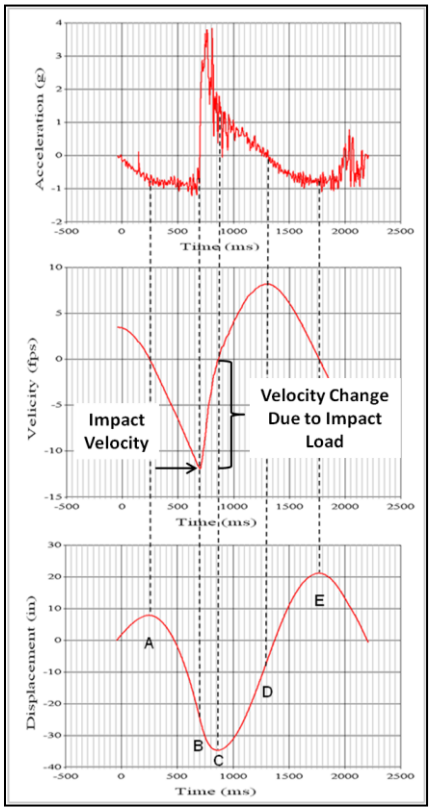

Figure 8. Wave Impact Sequence of Events

The period of time in Figure 8 from point B to point C is the wave impact period, i.e., the shock pulse. It is this period of time from B to C that is important for understanding and

evaluating the effects of wave impacts. Five parameters are important for quantifying and characterizing an acceleration shock pulse, including direction, pulse shape, rate of acceleration application (i.e., jerk), peak amplitude, and pulse duration, *Eiband (1959).*

Consistent Wave Slam Type

The time history responses of individual wave slams tend to follow three characteristic patterns before and after the wave impact phase. The patterns are used to characterize types of wave impacts referred to as Alpha, Bravo, and Charlie wave slams, *Riley et al. (2010)*. The Type Alpha slam is one where the craft is airborne prior to impact. The stern of the craft impacts the water first and this induces bow down pitching just prior to a severe wave impact. The Type Bravo slam is one where the craft may be airborne or the stern stays in the water, and impact occurs with little or no bow down pitching prior to impact. Prior to impact there is typically a temporary loss of forward momentum for Type Alpha and Bravo slams. The Type Charlie slam is one where the craft is in the water, there is no loss of forward momentum. There is little or no bow-down pitching prior to impact and the impact causes rapid bow up pitching. The significance here is that even in what is sometimes described as a chaotic and random seaway in fully developed seas, the response motions observed in craft follow repeatable patterns.

Consistent Shock Pulse Shape

At any measurement point on a craft the direction of the shock pulse during a wave slam can be aligned with coordinate axes X (surge acceleration, positive forward), Y (sway acceleration, positive to port), and Z (heave acceleration, positive up). The shape of the rigid body vertical acceleration when impact forces dominate can be simplified for analytical study as a half-sine pulse, *Riley and Coats (2012)*. Figure 9 illustrates the half-sine representation of the rigid body vertical acceleration pulse for a wave impact where the largest amplitude is A_{max} and the pulse duration is T. While the sequence of wave encounters in terms of wave height and time between impacts is random, the vertical response of the craft to a single wave impact appears to be consistent and repeatable in shape with amplitudes that vary primarily with speed, craft weight, wave period, and wave height, *Riley, Coats, and Murphy (2014b).*

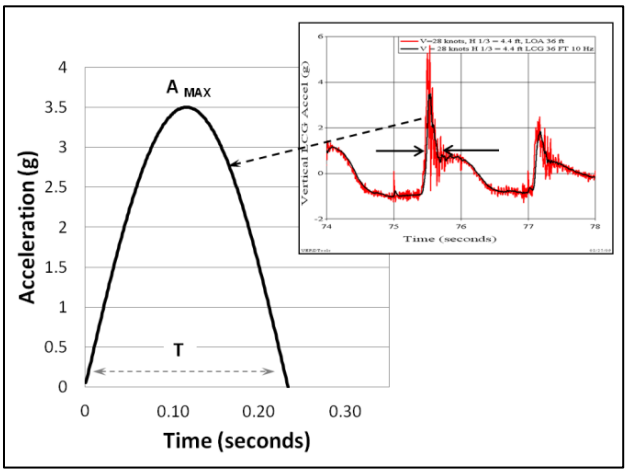

Figure 9. Half-sine Pulse Shape

Average Peak Acceleration Trends

The plot in Figure 10 shows a triangle for different seakeeping trials of 10 craft that weighed from 22,000 pounds (lbs) to 38,000 lbs. The acceleration value next to each triangle is the $A_{1/100}$ value for that run computed using *StandardG*. The solid lines are empirical data fits that trend with the data. The plot shows that for these craft the computed $A_{1/100}$ values increase and trend consistently as a function of craft average speed and significant wave height. This is another illustration of how craft responses to wave impacts are not random or chaotic. The wave heights vary randomly in time for a given sea state, but the craft's response (in this case average response) to wave impacts follows consistent trends. Appendix B presents additional details on the craft in the data base and presents the empirical equations useful for predicting $A_{1/10}$ and $A_{1/100}$ for different size craft.

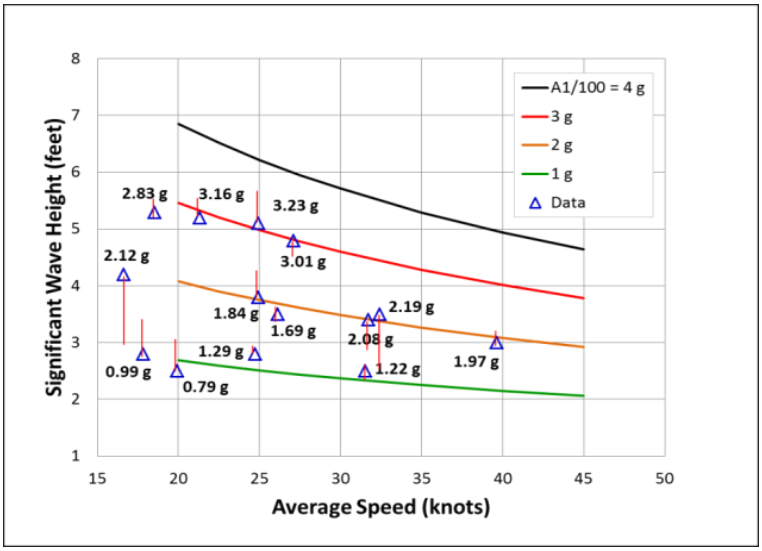

Figure 10. A1/100 Trends with Average Speed and Wave Height

Shock Pulse Duration

Figure 11 is a plot of wave impact duration versus peak acceleration recorded at the LCG in 13 different craft during head-sea trials in rough water, *Riley, Haupt, and Murphy (2014c)*. All wave impacts with peaks greater than 3 g where analyzed. Lower amplitude pulses were surveyed for trends. The squares in the figure correspond to six craft that weighed from 22,000 pounds to 38,000 pounds. The circles correspond to six craft that weighed from 14,000 pounds to 18,000 pounds. The triangles were recorded on a craft that displaced 105,000 pounds. The peak acceleration is the rigid body peak acceleration estimated using a 10-Hz low-pass filter. The data indicates that the shortest impact durations regardless of impact severity are on the order of 100 milliseconds (ms), and the longest durations decrease from about 450 ms to 150 ms as peak acceleration increases to about 7 g. The variation in the impact duration for a given peak acceleration is caused by several variables, including craft weight, speed, wave height, impact

angle, deadrise, and where the craft impacted the wave (e.g., on the leading flank, crest, or following flank).

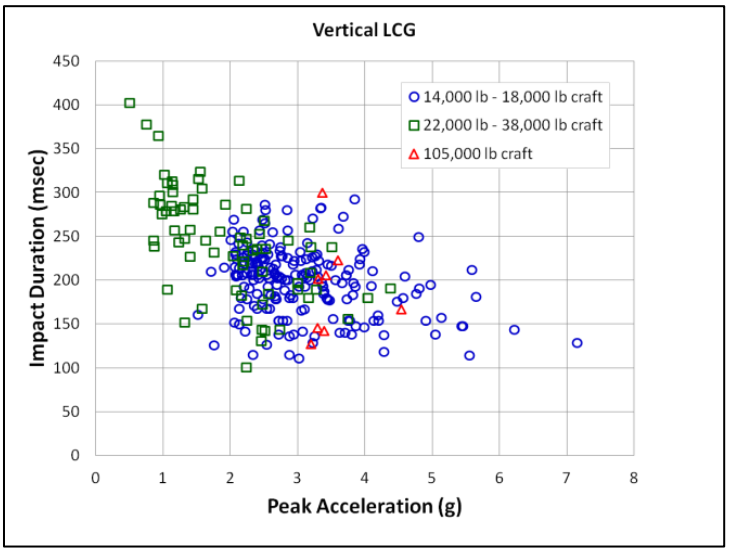

Figure 11. Wave Impact Shock Pulse Duration

Shock Response Spectrum

Figures 9, 10, and 11 illustrate how acceleration data recorded during seakeeping trials is used to characterize wave impact load in terms of pulse shape, amplitude, and duration. Once those characteristics have been identified, the individual shock pulse can be used for estimating shock effects on structure, equipment, or human comfort. One of the most useful mathematical tools for evaluating shock effects is the shock response spectrum (SRS). A shock response spectrum is the calculated maximum response of a set of single-degree-of-freedom, SDOF, spring-mass-damper oscillators to an input acceleration. Figure 12 illustrates the SRS concept for SDOF natural frequencies from 5 Hz to 40 Hz. The natural frequency of each SDOF is a function of its mass (m) and stiffness (k) as shown in equation (2).

$$f = \frac{\omega}{2\pi} = \left(\frac{1}{2\pi}\right)\sqrt{\frac{k}{m}} \quad \text{Hz} \qquad \text{Equation (2)}$$

The input acceleration is applied to the base of all oscillators, and the calculated maximum response of each oscillator versus the natural frequency make up the spectrum, *Harris (1995)*. The equations for predicting the responses are found in numerous engineering handbooks and *ISO-18431-4 (2007)*.

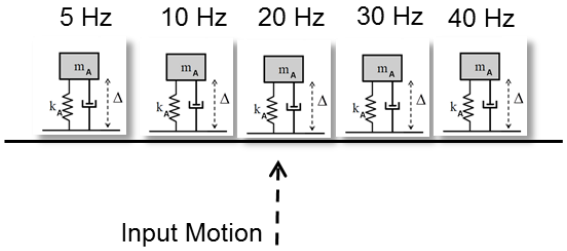

Figure 12. Shock Response Spectrum Concept

The predicted responses can be in terms of the maximum absolute acceleration of the mass, the maximum relative displacement (Δ) of the spring-damper assembly, or a relative velocity term. The maximum relative displacement is an intuitive parameter for potential shock damage because the maximum relative displacement across the spring is proportional to the strain in the spring. The shock pulse that results in the largest strain in the spring is the most severe shock pulse with the largest damage potential. Examples of the use of SRS to evaluate wave slam effects are presented in the next section. Appendix C presents additional information on shock response spectra, including the maximum acceleration SRS (ASRS) and the pseudo-velocity SRS (PVSRS).

An Integrated Approach

Physics-Based Methods

The repeatability of pulse shapes and types of wave slams and the trending of $A_{1/N}$ values with speed and wave height provide the motivation for studying the physics of individual wave impacts, but not at the expense of the wealth of knowledge accumulated from statistical approaches. Both approaches are needed, especially in light of the inability to measure individual wave heights during seakeeping trials. Relating the craft acceleration responses to the seaway environment requires $A_{1/N}$ and $H_{1/N}$ statistics. When both deterministic and statistical approaches are applied they provide lessons learned for addressing a broader range of design and comparative analysis topics than obtained from just one approach. But the fundamental physics of individual impacts must be understood before statistical methods are applied to expand analysis capabilities from single impacts to multiple impacts.

Figure 13 illustrates the taxonomy for conceptualizing an integrated approach to studying wave slam effects on high speed craft. The goal is to apply a common approach to defining wave impact load for studying effects on structure, equipment, and humans with knowledge from both deterministic and statistical approaches depending upon the level of physical complexity. Level I studies individual wave impacts to gain basic understanding of the physical phenomena and the mathematical models that best describe the physics.

Level II extends the knowledge base by investigating how combined effects of multiple impacts of equal severity affect outcomes. Level III adds the complexity of differing sea

conditions and what maximum loading conditions can be expected. It is important to note that the end products of applied research may not have to evolve through all three phases. For example, a design approach based on a single severe shock pulse may not require Level II or III studies. The following examples show how the Figure 13 integrated approach can be implemented.

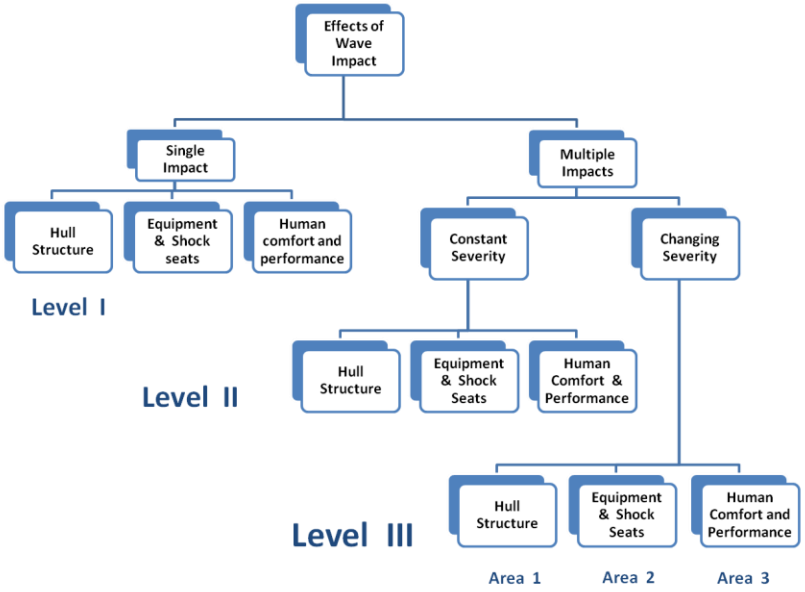

Figure 13. An Integrated Approach to Studying Wave Slam Effects

Hull Design Acceleration

In early hull design studies the static equivalent of the dynamic load acting on the bottom of a craft hull was defined as the static pressure which produces the same maximum strain in a structural element as the dynamic load, *Heller and Jasper (1960)* and *Allen and Jones (1978).* Several assumptions can be used in a deterministic approach to transition this definition to an equivalent static acceleration, *Riley and Coats (2012).* The first assumption is that the vertical dynamic acceleration at a cross-section of a craft has the shape of a half-sine pulse given by equation (3) where the pulse duration in this equation is T/2.

$$A(t) = A_{MAX} \sin\left(\frac{2\pi t}{T}\right) \tag{3}$$

The second assumption is that there is an equivalent average acceleration $\overline{A}(t)$ with a rectangular (or square) pulse shape and maximum amplitude given by equation (4) that produces

the same strain in a structural element (i.e., equivalent damage potential) as the half-sine pulse given by equation (3).

$$\overline{A} = \frac{A_{MAX}}{T/2}\int_0^{T/2} \sin\left(\frac{2\pi t}{T}\right) dt = \frac{2}{\pi} A_{MAX} \tag{4}$$

The equivalency of the $A(t)$ half-sine pulse and the $\overline{A}(t)$ rectangular pulse can be demonstrated by comparing the maximum relative displacement SRS (DSRS) of each pulse.

Figure 14 compares the DSRS for three different pulses shown in the insert. One pulse is a 5g – 200 msec half-sine acceleration pulse (triangle symbol) that represents a wave impact shock pulse. The 3.18g – 200 msec rectangular pulse (grey circles) has the same 200-msec duration with a reduced constant 3.18 g amplitude computed using 5 g in equation (3-2) . The predicted DSRS curves for the 200-msec pulses above 10 Hz are nearly identical, indicating the 5 g – 200 msec half-sine pulse and the 3.18 g – 200 msec rectangular pulse have the same damage potential for response modes above approximately 10 Hz (i.e., they are equivalent severity pulses).

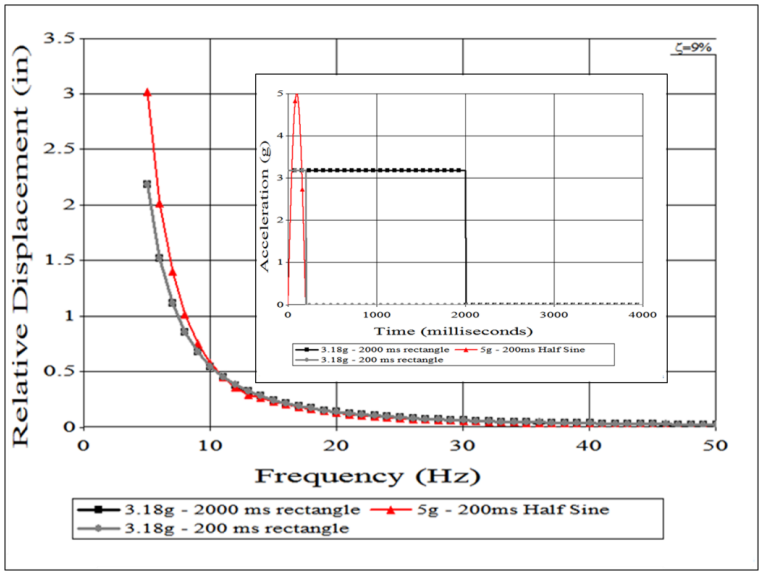

Figure 14. Relative Displacement SRS for Half-Sine and Square Pulses

The 3.18 g - 2000 msec pulse (black squares) is also included to explain the concept of an equivalent static pulse. Typically the word static elicits the thought of a constant phenomenon with infinite duration, but in structural dynamics, where a maximum strain value is of interest, a load with short duration (e.g., 200 msec) can produce the same maximum strain as a lower amplitude load whose duration is much longer. As the duration of the pulse increases, the maximum strain responses in the spring do not change because they occurred early in the response time (in this case within the first 200 msec). As long as the maximum strain occurs

within the duration of the half-sine acceleration pulse, the DSRS are the same (i.e., the maximum strains are the same). In the limit, as the rectangular pulse duration becomes large (i.e., approaches static) the maximum relative displacements (i.e., strain) for all natural frequencies of interest remain constant. The concept of static equivalency can be used for high speed planing craft because structural frequencies are typically greater than 15 Hz with corresponding periodic response times on the order of 66 msec and less (i.e., short compared to the relatively long wave impact durations).

When a maximum shock pulse for a single wave slam (i.e., the design severity pulse) is modeled as a half-sine pulse, equation (4) can be used to calculate its equivalent static acceleration. The equivalent static acceleration (i.e., the load impact factor) can be used in developing hull design methods similar to the *Allen and Jones (1978)* method.

The hull design approach is to consider a single most severe shock pulse and to design the hull with appropriate margin to withstand that pulse. In Figure 13 this is a Level I approach. If multiple impacts over long periods of time were considered in a fatigue analysis study it would be a Level II (constant severity) or Level III (varying severity) study.

Equipment Ruggedness Testing

The DSRS (or PVSRS or ASRS) can also be used to establish laboratory testing criteria for minimizing the risk of equipment failure or malfunction while operating in a wave slam environment. For example, when a single long-duration wave slam pulse is selected as a maximum shock pulse (i.e., Level I approach), its DSRS can be compared to the DSRS of a shorter duration laboratory shock machine pulse to ensure the laboratory pulse is more severe than the wave slam pulse. The plot on the left in Figure 15 shows a wave impact shock pulse with duration equal to 120 msec (red curve, triangle symbol) and a shock machine pulse with a 23-msec duration (blue smooth curve). The plot on the right shows the relative displacement DSRS for the two shock pulses. The DSRS curve for the shock machine pulse (blue smooth curve) is greater than the DSRS for the wave shock pulse (red curve, triangle symbol) for natural frequencies greater than 10 Hz. Since the shock machine pulse is more severe it can be used to test hard mounted equipment (with natural response modes greater than 10 Hz) in the laboratory before installation in a craft.

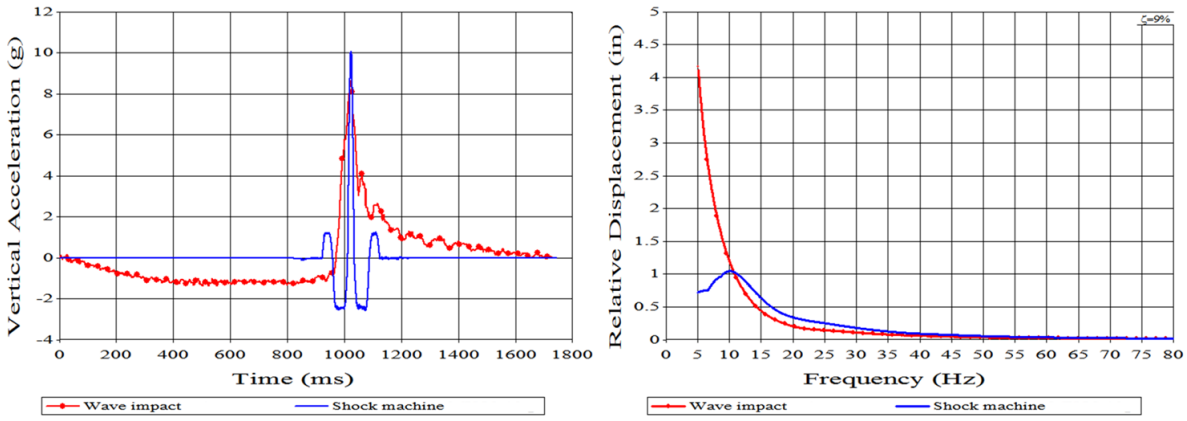

Figure 15. Example SRS for Laboratory Shock Test Machine

Another damage mode for equipment over long periods of time that can cause malfunction involves disconnects of plugs or circuit cards (i.e., friction fits). A laboratory test that mitigates the potential for this type of failure could be a series of hundreds of low severity shock pulses spaced at equal time intervals like repeated wave impacts (i.e., a Level II approach in Figure 13).

Shock Isolation

Experience has demonstrated that shock isolation systems with improper frequency for the spring-damper assembly can lead to shock amplification (i.e., even without bottoming) in high-speed craft rather than shock mitigation. This is true for both shock isolation seats and equipment shock isolation mounts.

We know from data like that shown in Figure 11 that wave slam pulse durations are on the order of 100 msec or more. This knowledge coupled with a SDOF model of a shock isolation system and a consistent half-sine acceleration pulse as the input to the SDOF model can help ensure that effective mitigation systems are achieved. This applies to design and selection of spring-damper assembly components as well as laboratory validation test procedures that demonstrate effective mitigation before operational use.

As an example of laboratory test method development, the half-sine acceleration pulse shape of a severe wave slam (i.e., the wave impact load) can be used to develop criteria for laboratory test and evaluation of shock isolation seats before installation in a craft, *Riley, Ganey, Haupt, Coats (2015b).* Assume that a 10 g – 100 msec half-sine acceleration pulse is selected to represent the maximum severity wave impact load (i.e., a Level I approach). An impact medium for a drop test can be selected to create a 10 g - 100 msec half-sine pulse upon impact. In addition, the change in velocity of this pulse (i.e., the area under the acceleration curve, approximately 20.5 feet per second) is equal to the drop-test impact velocity, which can be used to calculate the planned test drop height (e.g., 6.5 feet for the 10 g – 100 msec shock pulse).

The DSRS of acceleration data recorded during the seat drop test can be used to compute a seat performance measure, *Riley et al. (2015c).* For example, if vertical accelerometers are installed at the base of the seat and on the seat pan, the recorded pulses can be used to compute the maximum relative displacement SRS for the base input and the DSRS of the pan response. A ratio of the DSRS can then be used to define a mitigation ratio that is a simple yet consistent measure of the percent reduction in the shock input to the seat.

Appendix D provides additional information on methods for selecting effective shock isolation systems.

Ride Comfort

The crew comfort and performance criteria listed in Table 1 were developed based on subjective crew feedback after being subjected to high-speed runs in varying sea states. Unfortunately there has been no systematic research performed to advance the state of the art in understanding or quantifying human comfort at sea, including the study of surge and sway accelerations and rapid pitch and roll effects. In the absence of dedicated research the only recent addition has been a refinement of the vertical acceleration criteria (i.e., $A_{1/10}$ values) based on recent crew feedback from rough water seakeeping trials. Many of the rough water trials recently analyzed included runs where the coxswain was directed to achieve a maximum safe speed in each heading with no throttling. Systematic analysis of archived data and subjective feedback

from the experienced test coxswains, test engineers, and naval architects participating in the trials resulted in an interesting observation. During the maximum safe speed runs in head seas (i.e., typically the most uncomfortable ride tolerated by the coxswain), the $A_{1/10}$ values varied from 2.7 g to 3.2 g, which correlated well with the 3-g extreme discomfort level in Table 1[3]. Table 2 lists this range with others that were developed based on recent test crew subjective feedback *(Riley, Ganey, Haupt, 2015a)*.

An example application of the statistical $A_{1/10}$ ranges from Table 2 is shown in Figure 16. The plot abscissa is a linear scale of all the peak accelerations largest to smallest output by StandardG for a test run. The ordinate is a logarithmic scale of the percent of peaks greater than or equal to that peak-g value (i.e., similar to a cumulative distribution in log format). Peak accelerations for two sets of data recorded during different seakeeping trials are shown. It illustrates a useful visual display of two very different rides. The upper curve was a ride that included wave slams that were described as extremely uncomfortable (i.e., some peak accelerations in the orange zone up to 5 g.) compared with another ride that was called an "easy day underway" (i.e., all peak accelerations in the green zone). The color shading corresponds to the transition zones listed in Table 2. On the logarithmic scale the value of 10 corresponds to 10 percent of the data, so all the peaks to the left of 10 percent were the peaks used to compute $A_{1/10}$ for that run. Likewise a value of 1 corresponds to 1 percent. All peaks to the left of 1 percent were the ones used to compute $A_{1/100}$.

Table 2. Interim Transition Zones for Human Comfort and Performance

$A_{1/10}$	Transition Zones
< 1.5 g	Conditions typically result in a comfortable ride with effective performance for 4 hours or more
1.5 g - 2.0 g	Conditions may transition from a comfortable ride to a ride with limited discomfort
2.0 g - 2.7 g	Conditions transition from a comfortable ride to a ride with discomfort and limited performance
2.7 g - 3.2 g	Conditions transition from discomfort to the onset of extreme discomfort
3.2 g - 5.5 g	Conditions transition from extreme discomfort to the onset of concern for personnel safety
5.5 g - 6.0 g	Conditions transition from extreme discomfort and concern into potentially unsafe conditions with increased risk of safety mishaps

[3] A single wave impact at 3g was described as "quite uncomfortable" in *Ducane (1956)*.

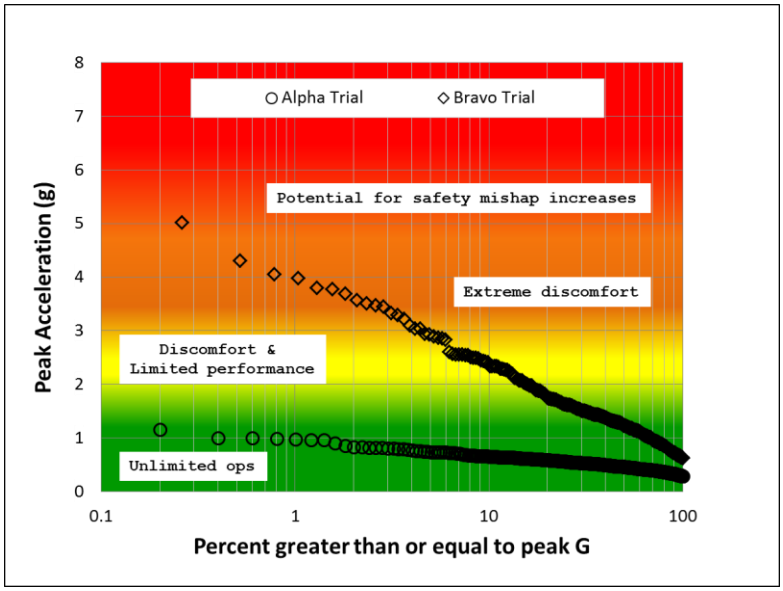

Figure 16. Ride Severity Profiles for Two Seakeeping Trials

Research Opportunities

The deterministic analysis of wave impacts offers a consistent engineering approach to defining impact loads that can be applied with common engineering rationale regardless of the topic of interest (e.g., structure, equipment, human comfort). It has the benefit of aligning maximum peak accelerations observed in testing with design loads and criteria with known design margins. The example applications presented herein are based primarily on vertical craft motions, so there is ample opportunity as summarized below for additional research and continued improvement.

Instrumentation

During full-scale seakeeping trials the response of a craft to wave impacts can be measured with good accuracy, including rigid body accelerations and rotations, vibration motions, strain, and craft speed just to name a few. Recording and interpreting impact pressure data is more difficult to the extent that the cost of installation precludes frequent attempts at the measurement. The independent variable that cannot be measured confidently at full-scale is the relative motion between the craft and each incident wave (either distance or velocity). The height of individual waves cannot be measured or correlated with individual peak acceleration responses. Development of a measurement sensor that could close this gap (e.g., either a displacement measurement or relative velocity measurement) would significantly improve understanding the cause and effect physics and modeling assumptions of different wave impacts.

Model Testing

It was hypothesized that irregular seas should be simulated “to determine the actual forces and motions that may truly be anticipated”, *Michel (1968)*. It is not clear that this hypothesis also applies to wave slam effects in small high-speed planing craft. A research opportunity therefore

exists to study wave impact responses on model scale. Wave heights in tank tests can be measured with good accuracy, and the variation of maximum impact acceleration with speed and wave period (just to name a few parameters) can be pursued in a deterministic approach. As an example, Figure 17 shows two test matrices where each triangle is a scale model run in a tank. Each matrix has a unique wave period. The goal is to investigate and model the mathematical relationship between the maximum wave slam severity (i.e., peak acceleration) and the three independent variables. This approach could potentially obviate the issue related to how many impacts are required for tank testing to calculate $A_{1/100}$ or $A_{1/10}$ [4], and it could be applied to other dependent variables like maximum surge acceleration and maximum pitch angle. It could also be used to investigate how craft motions transition from Type Charlie slams, to Type Bravo slams, to Type Alpha slams as speed and wave height increases.

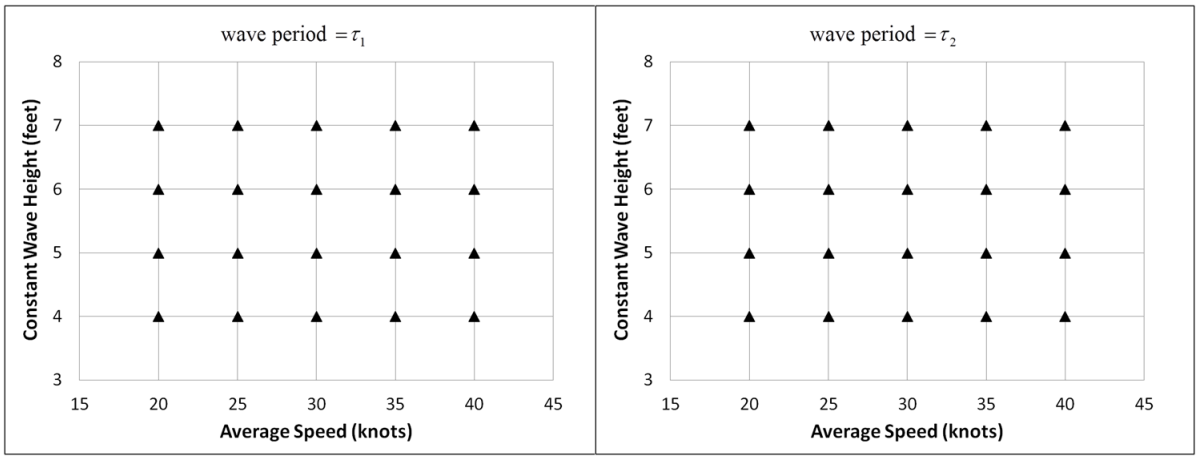

Figure 17. Scale-model Test Matrices

Knowledge of how peak accelerations vary with speed and constant wave height as shown in Figure 17 seeks first to understand individual wave impact characteristics (i.e., Level I in Figure 13). This tow-tank study could then be expanded to a Level III study for predicting impact severities that vary over time using statistical models of exponential, Raleigh, or log-normal wave distributions.

Hull Design

Assumptions related to effective bottom pressure loads and impact load factors have resulted in tractable design approaches for the very complicated dynamic environment of small high-speed planing craft. However, the dichotomy of designing hulls with less than a maximum operational load (e.g., use of $A_{1/100}$, the average of the top one percent of wave impact loads rather than A_{MAX}) suggests that published planing hull design equations have unknown safety factors or margins that result in maximum environmental loads. Published equations are useful, but the unknown margins leave no room for flexible hull design optimization by individual

[4], Observation shared during private discussion with Donald Jacobson, Code 831, Naval Architecture Branch, Combatant Craft Division, Naval Surface Warfare Division Carderock s in 2013.

designers. There is an opportunity for research that unravels the dichotomy and better defines equations with known allowances for design margins.

Human Comfort and Performance

Table 2 is a rough estimate of how human discomfort and reduced performance varies with increasing vertical acceleration amplitudes. Although recent personnel feedback correlates well with the historical descriptions of comfortable rides and extreme discomfort, the current descriptions at the high end are broad, and it is well known that transverse accelerations and multi-axis rotations can also cause extreme discomfort. There is a need for systematic research for effects other than vertical, and there is a need for controlled studies to better describe and quantify the bounds of human discomfort. This knowledge will improve the ability to set operational limits that avoid the more severe environments that transition into unsafe conditions.

The 3.2-g value at the upper end of the extreme discomfort zone in Table 2 has no current basis in human comfort research. It is a rough estimate based on the perceptions and feedback of skilled test coxswains. The equivalent static acceleration from equation (4) for a 3.2-g half-sine pulse is 2 g, but the question remains, is some other equivalent static value like 2.5 g more appropriate. Additional human comfort research is required to establish test-based rationale for defining the transition zones listed in Table 2.

Conclusions and Recommendations

The development of computational methods for high-speed craft hull design and human comfort evolved with a reliance on statistical parameters to quantify the wave impact environment. This was a natural evolution dealing with wave heights in irregular seas best characterized by statistical methods and the evolution of computer data processing in the 1970’s and 1980’s. Across diverse communities of interest however, different statistical approaches for processing recorded acceleration data were developed for different applications that have no common engineering rationale or consistency in the metrics for quantifying wave impact load.

More recent advancements in general purpose data analysis software speeds the process of analyzing acceleration data and allows a focus on studying responses to individual wave impacts. This has revealed interesting observations related to elements of wave slam response repeatability even in a random wave environment. Instead of the statistical averaging of many impacts, the deterministic approach has provided improved understanding of the cause and effect physics of individual wave impacts and allows for consistent engineering rationale to be applied for studying wave impact effects.

The primary focus of recent deterministic studies has been on the vertical inputs and responses in high-speed craft. It is recommended that the deterministic approach also be pursued in studying other important response motions (e.g., surge and sway impact components, as well as pitch and roll effects).

The pursuit of individual wave impact knowledge should not be at the expense of the wealth of knowledge accumulated from statistical studies. Both approaches are needed, especially in light of the inability to measure individual wave heights in the open ocean environment. Craft motion responses in a seaway over time can be described using statistical

methods; however the response of a craft to single wave impacts must first be understood. When both deterministic and statistical approaches are applied they provide lessons learned for addressing a broader range of design and comparative analysis topics than obtained from just one approach. It is therefore recommended that further deterministic research be pursued by numerous organizations to expand the knowledge base in craft motion mechanics and wave slam effects on hull structure, equipment, and human comfort.

REFERENCES

ALLEN, R.G., JONES, R.R. (1978). *A Simplified Method for Determining Structural Design-Limit Pressures for High performance Craft*, American Institute of Aeronautics and Astronautics, Society of Naval and Marine Engineers Advanced Marine Vehicle Conference, 78-754, April 1978.

BOILEAU, P.E., TURCOT, D., SCORY, H. (1989). *Evaluation of Whole-Body Vibration Exposure Using a Fourth Power Method and Comparison with ISO 2631*, Journal of Sound and Vibration, 129(1), 1989.

BLOUNT, D. L. (2014). *Performance by Design, Hydrodynamics for High-Speed Vessels*, First printing, ISBN 0-978-9890837-1-3, Virginia Beach, Virginia, USA

DUCANE, P. (1956). *The Planing Performance, Pressures, and Stresses in a High-Speed Launch*, Presented in London at a Meeting of the Institution of Naval Architects, 7 June 1956.

DUCANE, P. (1971). *Fast Patrol Boats*, Symposium on Small Craft, Southampton, England, UK, 1971.

EIBAND, M. (1959). *Human Tolerance to Rapidly Applied Accelerations: A Summary of the Literature*, Lewis Research Center, National Aeronautics and Space Administration, Memorandum 5-19-59E, Cleveland, Ohio, June 1959.

ELLSWORTH, W.M. (1974). *Hydrofoil Development – Issues and Answers*, AIAA/SNAME Advanced Marine Vehicles Conference, San Diego, California, USA.

FRIDSMA, G. (1971) *A Systematic Study of the Rough Water Performance of Planing Boats –(Irregular Waves) – Part II*, Research Report 1495, Davidson Laboratory, Stephens Institute of Technology, Hoboken, N.J., USA, March 1971.

HARRIS, C.M., editor-in-chief (1995). *Shock and Vibration Handbook, Fourth Edition*, McGraw-Hill Companies, Inc., New York, New York, 1995.

HELLER, Jr., S.R. and JASPER, N.H. (1960). *On the Structural Design of Planing Craft*, Quarterly Transaction, Royal Institute of Naval Architects, July 1960.

HOGGARD, M.M., JONES, M.P. (1980). *Examining Pitch, Heave, and Accelerations of Planing Craft Operating in a Seaway*, High-Speed Surface Craft Symposium, Brighton, England, June 1980.

ISO-18431-4: 2007, *Mechanical vibration and shock – Signal processing – Part 4: Shock response spectrum analysis*, International Organization for Standardization, Geneva, Switzerland, 2007.

ISO-2631/1-1985(E), *Mechanical vibration and shock – Evaluation of human exposure to whole-body vibration – Part 1: General requirements*, International Organization for Standardization, Geneva, Switzerland, 1985.

ISO-2631-1: 1997 (E), *Mechanical vibration and shock – Evaluation of human exposure to whole-body vibration – Part 1: General requirements*, International Organization for Standardization, Geneva, Switzerland, 1997.

ISO-2631-5: 2004 (E), *Mechanical vibration and shock – Evaluation of human exposure to whole body vibration – Part 5: Method for Evaluation of Vibration Containing Multiple Shocks*, International Organization for Standardization, Geneva, Switzerland, 2004.

JACOBSON, A., COATS, T., HAUPT, K., POGORZELSKI, D., JACOBSON, D. (2007). *Working Towards Vertical Acceleration Data Standard*s, Maritime Systems and Technology (MAST) Contone Congressi, Porto Antico, Genoa, Italy, 14 – 16 November 2007.

KOELBEL, Jr., J.G. (2001*). Structural Design for High Speed Craft Part II*, Professional Boat Builder, Number 68, pages 32 – 43, December/January 2001.

MANTZ, P. A., COSTANZO, F. A. (2009). *An Overview of UERDTools Capabilities: A Multi-Purpose Data Analysis Package*, Proceedings of the IMAC-XXVII Conference and Exposition on Structural Dynamics, Society of Experimental Mechanics, Inc., Orlando, Florida, USA, 9-12 February 2009.

MICHEL, W. H. (1968). *Sea Spectra Simplified*, The Society of Naval Architects and Marine Engineers, Marine Technology, January 1968.

MUNK, W. H. (1944). *Proposed Uniform Procedure for Observing Waves and Interpreting Instrument Records*, Scripts Institute of Oceanography Wave Report 26, December 1944.

NASA (1972). *Symposium on Vehicle Ride Quality*, held at Langley Research Center, Hampton, VA, 6-7 July 1972, National Aeronautical and Space Administration, NASA Technical Memorandum TM X-2620, October 1972.

PETERSEN, R., PIERCE, E., PRICE, B., BASS, C. (2004). *Shock Mitigation for the Human on High Speed Craft: Development of an Injury Impact Design Rule*, paper presented at the RTO AVT Symposium on Habitability of Combat and Transport Vehicles: Noise, Vibration and Motion, Prague, Czech Republic, 4 – 7 October 2004.

PICKFORD, E.V., MAHONE, R.R., WOLK, H.L. (1975). *Slam/Shock Isolation Pedestal*, United States Patent Number, 3,912,248, 14 October 1975.

RILEY, M. R., HAUPT, K. D., JACOBSON, D. R. (2010a). "A Generalized Approach and Interim Criteria for Computing $A_{1/n}$ Accelerations Using Full-Scale High Speed Craft Data", Naval Surface Warfare Center Carderock Division Report NSWCCD-23-TM-2010/13, April 2010.

RILEY, M., COATS, T., HAUPT, K., JACOBSON, D. (2010b), *The Characterization of Individual Wave Slam Acceleration Responses for High-Speed Craft*, Proceedings of the American Towing Tank Conference, Annapolis, Maryland, August 2010.

RILEY, M. R., COATS, T.W. (2012). *Development of a Method for Computing Wave Impact Equivalent Static Accelerations for Use in Planing Craft Hull Design*, The Society of Naval Architects and Marine Engineers, The Third Chesapeake Powerboat Symposium, Annapolis, Maryland, USA, June 2012.

RILEY, M.R., COATS, T. W., MURPHY, H. P. (2014a). *Acceleration Response Mode Decomposition for Quantifying Wave Impact Load in High-Speed Planing Craft*, Naval Surface Warfare Center Carderock Division Report NSWCCD-80-TR-2014/07, April 2014.

RILEY, M. R., COATS, T. W., MURPHY, H. P. (2014b). *Acceleration Trends of High-Speed Planing Craft Operating in a Seaway*, Society of Naval Architects and Marine Engineers, The Fourth Chesapeake Powerboat Symposium, Annapolis, Maryland, USA. 23-24 June 2014.

RILEY, M., HAUPT, K., MURPHY, H., (2014c). "An Investigation of Wave Impact Duration in High-Speed Planing Craft", Naval Surface Warfare Center Carderock Division Report NSWCCD-80-TR-2014/26, April 2014.

RILEY, MICHAEL R., GANEY, DR. H. NEIL., HAUPT, KELLY, (2015a). "Ride Severity Profile for Evaluating Craft Motions", Naval Surface Warfare Center Carderock Division Report NSWCCD-80-TR-2015/002, January 2015.

RILEY, M. R., GANEY, H. N., HAUPT, K., COATS, T. W., (2015b). *Laboratory Test Requirements for Marine Shock Isolation Seats*, Naval Surface Warfare Center Carderock Division Report NSWCCD-80-TR-2015/010, May 2015.

RILEY, M. R., COATS, T. W., MURPHY, H. P., GANEY, H. N., (2015c). *A Method to Quantify Mitigation Characteristics of Shock Isolation Seats before Installation in a High-Speed Planing Craft*, The Society of Naval Architects and Marine Engineers, SNAME World Maritime Technology Conference, Providence, Rhode Island, 3 – 6 November 2015.

SAVITSKY, D., BROWN, P. (1975). *Procedures for Hydrodynamic Evaluation of Planing Hulls in Smooth and Rough Water, presented to the Hampton Roads Section, SNAME, Norfolk, Virginia, USA, 26 November 1975*.

SAVITSKY, D., BROWN, P. (1976). *Procedures for Hydrodynamic Evaluation of Planing Hulls in Smooth and Rough Water, Marine Technology*, Volume 13, No. 4, October 1976.

SAVITSKY, D., KOELBEL, J. (1978). *Seakeeping Considerations in Design and Operation of Hard Chine Planing Hulls*, Prepared for Combatant Craft Engineering Department, Naval Ship Engineering Center, Norfolk, Virginia, 17 May 1978.

SAVITSKY, D., KOELBEL, J. (1993). *Seakeeping of Hard Chine Planing Hulls*, SNAME, Technical and Research Bulletin No. R-42, June 1993.

STARK, D.R. (1980). *Ride Quality Characterization and Evaluation in the Low Frequency Regime with Applications to Marine Vehicles*, Conference on Ergonomics and Transport, Swansee, UK, 1980.

THIS PAGE INTENTIONALLY LEFT BLANK

APPENDIX A. SELECTION OF LOW-PASS CUTOFF FREQUENCY

Cutoff Frequency

Figure A-1 shows the amplitude functions for 2-pole and 4-pole Butterworth low-pass filters. The amplitude reduction at the cutoff frequency is equal to $1/\sqrt{2}$ (i.e., 0.707) [A-1]. The cutoff frequency for each calculated curve in the figure was set at 10 Hz. The amplitude scale is set to 1.0 at 0 Hz (i.e., direct current) to illustrate the attenuation provided by each filter. The frequency scale represents different frequencies in the acceleration signal. It is important to note that the 10-Hz low-pass filter does not pass all frequency content below 10 Hz nor does it remove all frequency content above the cutoff. This is characteristic of all low-pass filters. For example, in Figure A-1 the 8-Hz content in an acceleration signal would be passed with reduction factors of 0.84 for the 2-pole filter (i.e., 16% attenuation) and 0.92 for the 4-pole filter (i.e., 8% attenuation). Likewise, frequencies above the cutoff frequency are not completely removed. The 2-pole filter has reduction factors at 20 Hz and 30 Hz of 0.24 and 0.062, respectively (i.e., 76% and 93.8% attenuation). For the 4-pole filter the reduction factors for 20 Hz and 30 Hz are 0.11 and 0.012, respectively (i.e., 89% and 98.8% attenuation). Experience has shown that a 4-pole Butterworth low-pass filter is effective for estimating rigid body content by attenuating vibration content above approximately 20 Hz.

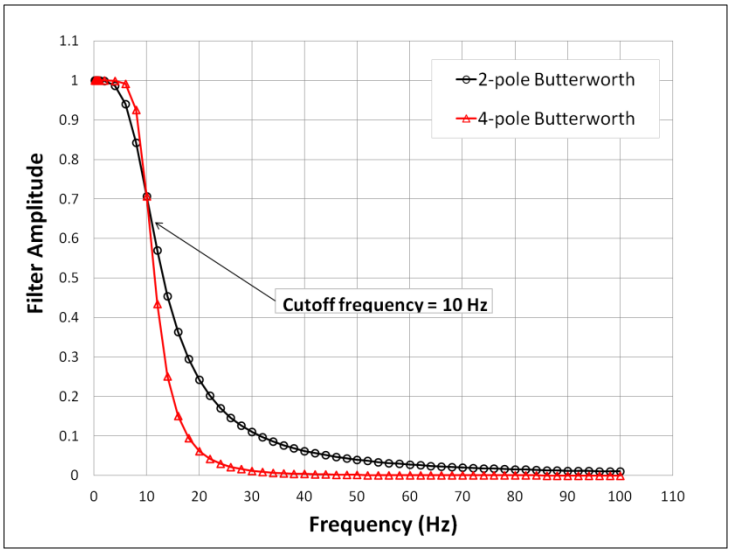

Figure A-1. Filter Amplitude Functions

Low-pass Filtering

The tutorial documents that describe the StandardG computational process suggest that a 10-Hz low-pass filter be used to extract peak rigid body vertical accelerations (i.e., heave accelerations) caused by wave impacts *unless some other cutoff value is indicated by frequency analysis (i.e., FFT analysis)* [A-2]. This is illustrated in Figure A-2 that shows the vertical acceleration recorded during two wave impacts in an aluminum 11-meter rigid-hull inflatable boat (RIB). The red curve is the unfiltered acceleration and the green curve is the 10-Hz low-pass filtered data. The 10-Hz cutoff value was confirmed by looking at the Fast Fourier Transform (FFT) plot of the entire acceleration record shown in Figure A-3.

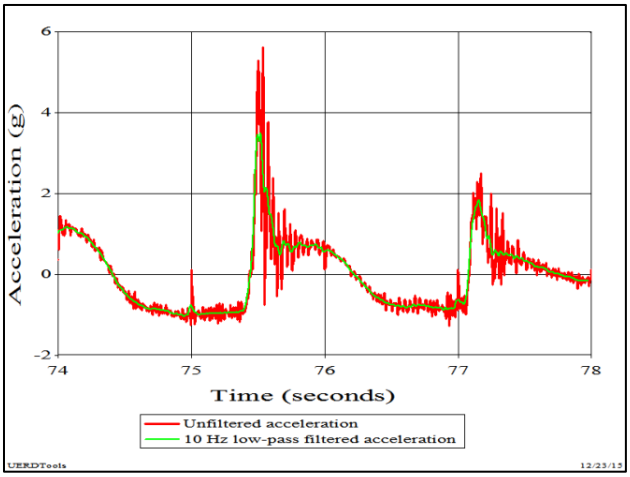

Figure A-2. Unfiltered and Low-pass Filtered Acceleration Data

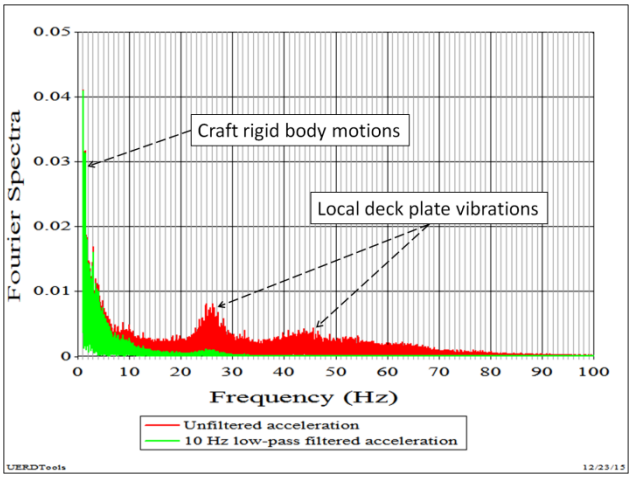

Figure A-3. Unfiltered and Low-pass Filtered FFT Plots

The Fourier transform converts the original acceleration signal into a summation of sinusoidal functions [A-3]. The FFT plots in Figure A3 show the relative amplitude of the different frequency sinusoids used to construct the original acceleration plot shown in Figure A-

2. The deck vibration content is shown by the humps in the red curve (i.e., the FFT for the unfiltered data) at approximately 25 Hz and 40 to 70 Hz. The FFT of the 10-Hz low-pass filtered acceleration data is the green curve. It clearly shows how the vibration content from 20 Hz to 70 Hz and higher has been significantly attenuated. The rigid body heave content in each signal is illustrated by the wave encounter frequency (i.e., the spikes below 2 Hz), and the varying wave impact pulse durations from roughly 1.25 Hz to 5 Hz (i.e., half-sine pulses with 0.10 to 0.40 second durations).

In Figure A-2 the phase delay caused by the low-pass filter has been removed by shifting the filtered record 0.0254 seconds to the left. The figure illustrates how proper selection of the low-pass cutoff frequency maintains the shape, amplitude, and duration of the acceleration pulse caused by the wave impact. For the impact pulse observed at approximately 75.5 seconds the rate of acceleration application (i.e., the acceleration jerk) is approximately the same for the filtered and unfiltered curves. The peak acceleration of the filtered curve is observed as a rough average of the high frequency oscillations, and the duration of the pulses (approximately 0.195 seconds) are approximately the same.

Cutoff frequencies less than 10 Hz are not typically recommended for high-speed craft data because of the possibility of a reduction in the indicated wave impact velocity (i.e., the area under the acceleration pulse). The following examples illustrate special cases where a cutoff frequency greater than 10 Hz was selected to attenuate vibrations and analyze structural responses in a high-speed craft.

Unique Deck Oscillations

Figure A-4 shows an example where a 30-Hz low-pass filter was used to evaluate unique motions of the deck of an 11 meter (m) cabin rib made of composite material. The plot shows a wave impact event that occurred in the time history at approximately 55.1 seconds. The red curve is the unfiltered acceleration recorded in the vertical direction at the base of a shock isolation seat. It shows an acceleration pulse from approximately 55.1 seconds to 55.24 seconds, followed by a negative seat-bottom impact spike at 55.24 seconds, and then low frequency deck oscillations in the 7-Hz to 9-Hz range.

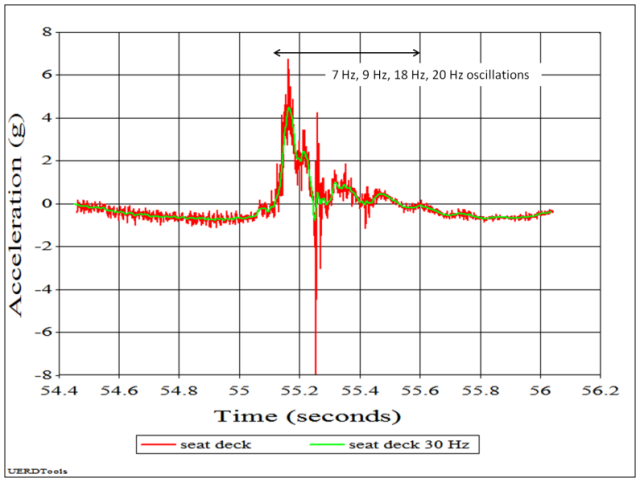

Figure A-4. Unique Deck Oscillation Using 30 Hz Low-pass Filter

During the wave impact, before the seat bottom impact, two cycles of deck oscillation are observed with periods that correspond to 18 Hz to 20 Hz. Analysis of other accelerations recorded at several deck and deckhouse locations indicated that the unique oscillations were caused by a composite deck house fore-aft flexural mode with dominant frequencies in the 17-Hz to 24-Hz range. After the seat bottom impact (i.e., at 55.24 seconds) the deck oscillations are observed to damp out with durations that correspond to approximately 7 Hz to 9 Hz. Analysis of other gage location data indicated the oscillations after the seat bottom impact were driven by a roughly 7-Hz to 8-Hz composite hull girder whipping mode. A 30-Hz low-pass filter was selected to analyze and quantify deck motions and shock isolation seat response motions after examination of the Fast Fourier Transform (FFT) plot shown in Figure A-5. The selection of the 30-Hz low-pass filter was based on the desire to remove vibration content above approximately 37 Hz and to retain the 7-Hz to 20-Hz deck motions caused by hull girder whipping and deck house flexure. The FFT plot in Figure A-5 shows how the 30-Hz low-pass filter attenuates the frequency content above 30 Hz and retains the majority of the 7-Hz to 20-Hz frequency content of interest.

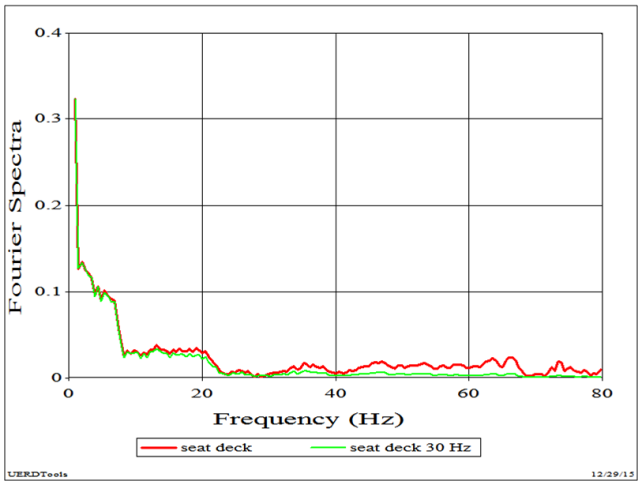

Figure A-5. FFTs of Unique Deck Oscillation and 30-Hz Low-pass Filtered Data

Over Filtering

Over-filtering occurs when a cut-off frequency is selected that is too low for the application. This can be detected by comparing the low-pass filtered acceleration data with the original unfiltered data in the time domain. Figure A-6 shows an example where a 10-Hz low-pass filter results in over-filtering the acceleration data. The red and green curves are the same unfiltered and 30-Hz low-pass filtered accelerations shown in Figure A-4. The dark blue curve is the acceleration time history after it was low-pass filtered using a 10-Hz cutoff frequency. The general characteristics of an over-filtered acceleration pulse, corresponding to the 10-Hz low-pass filtered data, include a reduced rate of acceleration application (i.e., jerk or acceleration slope), a reduced peak acceleration that does not average through the high frequency vibration oscillations, and an increased pulse duration. The light blue curve is for a 5-Hz low-pass filter to further illustrate the effects of over-filtering.

Figure A-7 shows the over filtering effects in the frequency domain (i.e., the FFT plot). The red curve is the FFT of the unfiltered acceleration data. The green curve is the FFT of the 30-Hz low-pass filtered data, the dark blue curve is the FFT for the 10-Hz low-pass filtered data, and the light blue curve is the FFT for the 5-Hz low-pass filtered data. The figure clearly shows how the 5-Hz and 10-Hz low-pass filters significantly attenuate the 7-Hz to 20-Hz frequencies of interest.

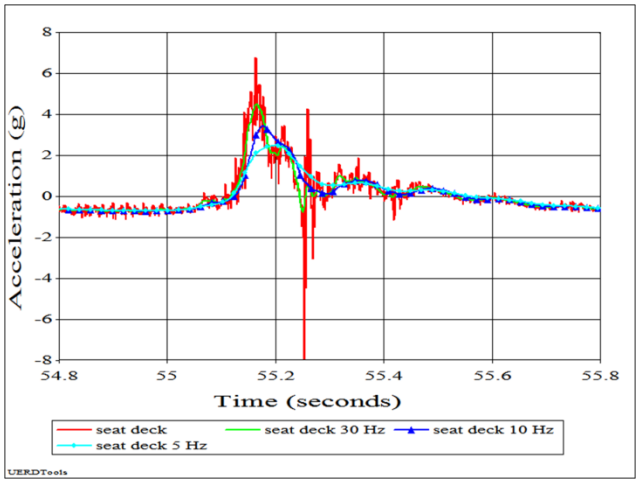

Figure A-6. Example of 10 Hz Low-pass Over-Filtered Acceleration Data

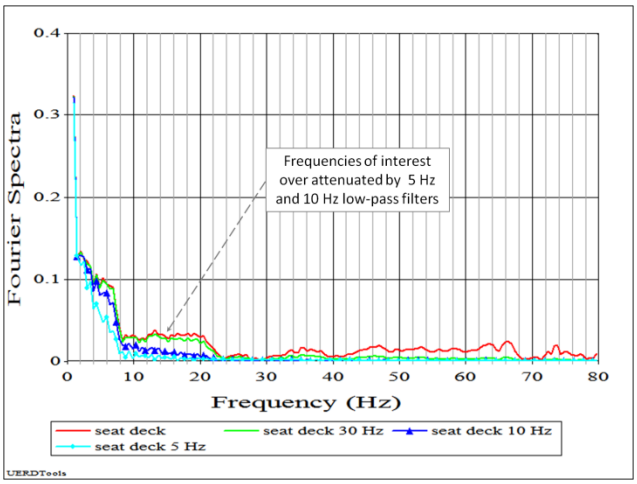

Figure A-7. Example 10-Hz Low-pass Over-Filtered FFT Plots

Acceptable Low-pass Filtering

As a general guide, there are four visual observations that can be used to conclude that acceptable low-pass filtering of an acceleration record has been achieved (i.e., no over filtering).

1. The rate of acceleration application (i.e., jerk) of the filtered record is approximately the same as the unfiltered record. See Figures A-4 and A-6.

2. The peak acceleration of the filtered record is observed to be approximately half-way between the vibration peaks and dips in the record. Depending upon the contiguous structure surrounding the gage position, the vibration signal during the impact (i.e., near the peak acceleration) may not be a symmetric signal with equal peaks and dips. See Figures A-4 and A-6.

3. The pulse duration of the low-pass filtered acceleration is approximately equal to the duration of the unfiltered acceleration. See Figures A-4 and A-6.

4. The maximum negative velocity of the filtered record is approximately the same as the maximum negative velocity of the unfiltered record. See Figure A-7.

In Figure A-7 the velocity curves for the unfiltered data (i.e., red curve) and the 30-Hz low-pass filtered data (i.e., green curve) are almost identical, indicating acceptable low-pass filtering. The changing slopes and changing negative peak amplitudes for the 5-Hz (i.e., light blue) and 10-Hz low-pass filtered data (i.e., dark blue) are indications of over-filtering.

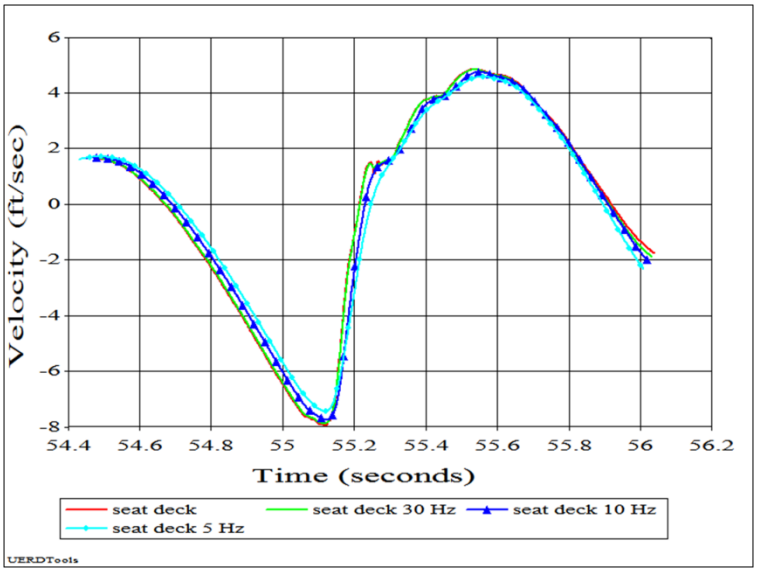

Figure A-7. Example of Over Filtered Velocity Plots

Appendix A References

A-1. Stanley, William D., Dougherty, Gary R., and Dougherty, Ray, *Digital Signal Processing*, Prentice-Hall, 1984.

A-2. Riley, Michael, R., Coats, Timothy, W., "A Simplified Approach for Analyzing Accelerations Induced by Wave Impacts in High-Speed Planing Craft", The Society of Naval Architects and Marine Engineers, The Third Chesapeake Powerboat Symposium, Annapolis, MD, 15-16 June 2012.

A-3. Webster, John, G., (1999). "The Measurement, Instrumentation, and Sensors Handbook", CRC Press LLC, Boca Raton, FL, USA.

Appendix B. Trends With Speed and Wave Height

Craft Full-Scale Data Base

The Combatant Craft Division of Naval Surface Warfare Center Carderock Division has conducted full-scale seakeeping trials of many craft since its establishment in 1967. The trials were not specifically focused on studying parametric effects on peak accelerations, but consistent testing protocols provide a sufficient data base for observing interesting trends. The investigation of these trends began under Office of Naval Research sponsorship to investigate acceleration data processing and data analysis methods, and has evolved into a broader study of craft motion mechanics and wave slam phenomena.

More than twenty different craft designs have undergone instrumented seakeeping trials between 1996 and 2014. Tri-axial accelerometers are often used but only the vertical data is presented. The data base summarized herein includes craft that weighed from approximately 14,000 pounds (6.35 metric tons) to 38,000 pounds (17.2 metric tons) with lengths that varied from 33 feet (10 meters) to 46 feet (14 meters). The range of average craft speeds and significant wave heights are shown in Figure B-1. Each data point corresponds to a single trial during which wave height and craft speed were measured. Wave buoy data is typically used to compute significant wave heights and average craft speeds are determined using global positioning systems. The craft where mostly deep-V hulls in the two weight categories listed in Table B-1. Trim and deadrise did not vary sufficiently within these subsets of data to result in observable trends.

Table B-1. Full-Scale Craft Characteristics

Craft Category	Craft Weight (lb)	Beam Loading Coefficient	L/B	Trim (deg)	Deadrise (deg)	$H^{1/3} / B$	$V / L^{1/2}$	Volume Froude Number
A	14,000 to 18,000	0.28 to 0.46	3.9 to 4.2	3 to 5	18 to 21	0.22 to 0.45	1.2 to 6.1	2.5 to 5.2
B	22,000 to 38,000	0.18 to 0.60	3.0 to 4.2	3 to 5	18 to 22	0.16 to 0.60	1.5 to 5.9	1.8 to4.0

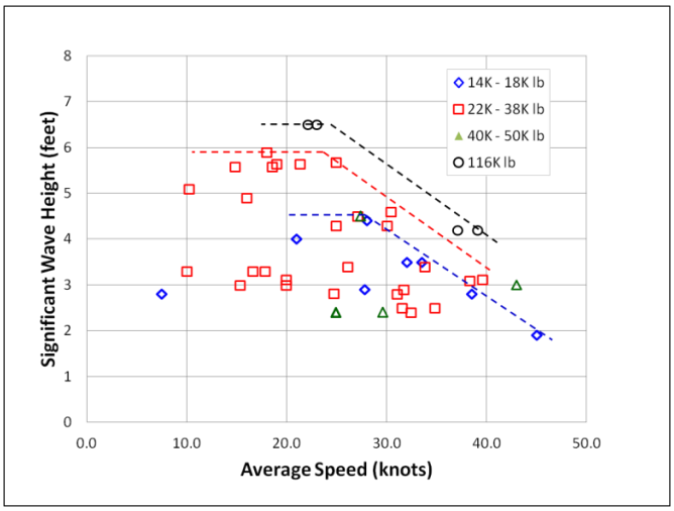

Figure B-1. Planing Craft Data Base Environmental Conditions

Data Processing

Archived acceleration data was analyzed using *StandardG* software to determine acceleration statistics, including root mean square (RMS), average, average of 1/3rd highest, average of 1/10th highest, average of 1/100th highest, and maximum peak accelerations. In all cases Fourier spectral analysis of raw signals indicated use of a 10-Hz low-pass filter was acceptable for extracting rigid body accelerations. The rigid body peak acceleration is a measure of the impact load in units of g.

In the following plots the data corresponds to head-sea conditions with short average wave periods between 3.4 seconds and 6.4 seconds. Observable trends in $A_{1/100}$ and $A_{1/10}$ values for Category A craft (i.e., 14,000 pounds to 18,000 pounds) are shown in Figure B2 and Figure B3, respectively. Craft lengths varied from 36 feet to 45 feet, and craft beams varied from 8.5 feet to 14.5 feet. The $A_{1/100}$ and $A_{1/10}$ value for each trial is shown plotted at the average craft speed and significant wave height for each trial. Category A is a very limited data subset (i.e., only 7 runs), so the trends are tentative pending availability of additional data. In Figure B-2 the rectangular bars correspond to ranges of uncertainty in the $A_{1/100}$ values due to less than 200 peak accelerations recorded during the trial.

The sensitivity analysis approach used to investigate trends within the data assumed that significant wave heights from wave buoy spectra could vary within 6-inches of computed values for varying sea spectra or during long duration runs. The red vertical lines indicate the uncertainty shift which resulted in the best fit is typically less than 6 inches.

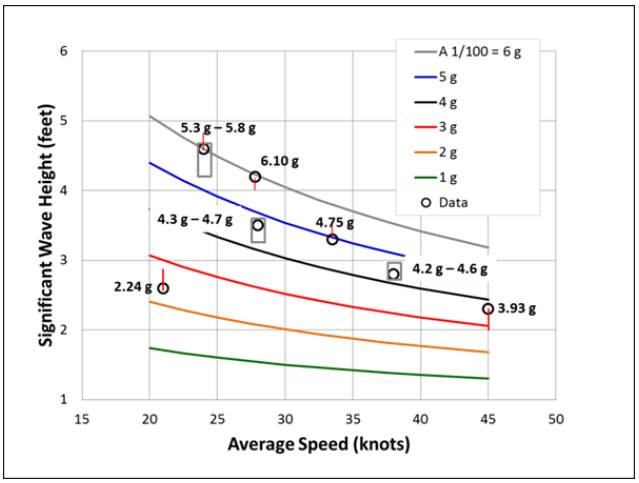

Figure B-2. $A_{1/100}$ Trends for Category A Craft

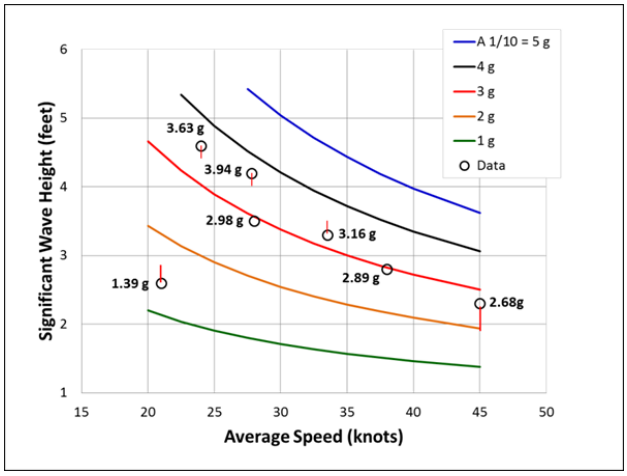

Figure B-3. $A_{1/10}$ Trends for Category A Craft

The lines of constant vertical acceleration in each plot were computed by the following best-fit equations for Category A craft.

$$A_{1/100} = \frac{(V_S + 12.63)(H_{1/3} - 0.73) - 11.14}{21.72} \qquad \text{Equation (B-1)}$$

$$A_{1/10} = \frac{(V_S + 0.77)(H_{1/3} - 0.70) - 5.52}{25.6} \qquad \text{Equation (B-2)}$$

$A_{1/100}$ and $A_{1/10}$ accelerations are at the LCG of the craft in units of g. V_s is average craft speed in knots and $H_{1/3}$ is significant wave height in feet.

Using this approach resulted in 5 of 5 craft in 7 of 7 runs trending within the uncertainty assumption with computed $A_{1/100}$ values from equation (B-1) within -7.0 percent to + 6.3 percent of $A_{1/100}$ data values.

Observable trends of $A_{1/100}$ and $A_{1/10}$ values with varying significant wave height and average speed for craft in Category B (i.e., 22,000 pounds to 38,000 pounds) are shown in Figure B-4 and Figure B-5, respectively. This is also a limited data subset (i.e., less than twenty runs), so the trends are tentative pending availability of additional data. Craft lengths varied from 33 feet to 48.9 feet and beams varied from 9 feet to 15 feet.

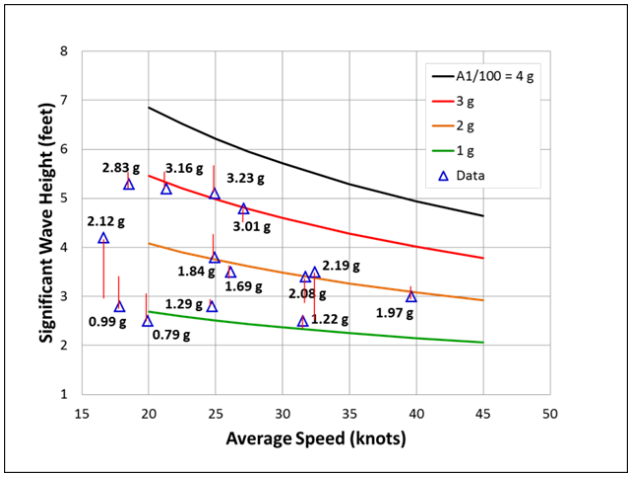

Figure B-4. $A_{1/100}$ Trends for Category B Craft

The lines of constant vertical acceleration in each plot were computed by the following best-fit equations for Category B craft. $A_{1/100}$ and $A_{1/10}$ accelerations are at the LCG of the craft in units of g. V_s is average craft speed in knots and $H_{1/3}$ is significant wave height in feet.

$$A_{1/100} = \frac{(V_S + 21)(H_{1/3} - 1.03)}{56.83} - 0.20 \qquad \text{Equation (B-3)}$$

$$A_{1/10} = \frac{(V_S + 7.46)(H_{1/3} - 1.08)}{62.5} \qquad \text{Equation (B-4)}$$

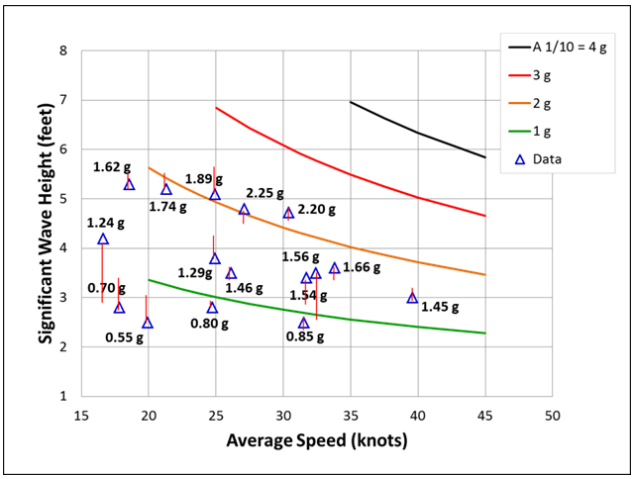

FigureB-5. $A_{1/10}$ Trends for Category B Craft

Using the sensitivity analysis approach with the uncertainty assumption resulted in 8 of 10 craft in 14 of 16 runs trending within the uncertainty assumption and resulted in computed $A_{1/100}$ values from equation (3) within -7.0 percent to + 6.3 percent of $A_{1/100}$ data values. For the computed $A_{1/10}$ values 8 of 10 craft in 16 of 18 runs trended within the uncertainty assumption and resulted in computed $A_{1/10}$ values from equation (B-4) within -11.1 percent to + 12.4 percent of $A_{1/10}$ data values. In Figures B-2 through B-5 each line of constant acceleration should be treated as a transition zone rather than an exact line on the plot.

The preliminary investigations of available data included searching for trends with craft displacement in the form of the volume Froude number. To date however a satisfactory equation has not yet been found that fits the combined data subsets (i.e., all weight values). Further investigations are required with a goal of developing one equation that fits all the data.

Appendix B References

B-1. Riley, Michael R., Coats, Timothy W., Murphy, Heidi P, *Acceleration Trends of High-Speed Planing Craft Operating in a Seaway*, Society of Naval Architects and Marine Engineers, The Fourth Chesapeake Powerboat Symposium, 23-24 June 2014, Annapolis, Maryland.

THIS PAGE INTENTIONALLY LEFT BLANK

APPENDIX C. SHOCK RESPONSE SPECTRUM

A shock response spectrum (SRS) is a computational tool used extensively to compare the severity of different shock motions [references C-1 to C-7]. Example applications include (1) comparing field shock test data to laboratory test machine data to ensure laboratory tests simulate the effects of shock pulses experienced under actual field conditions, (2) comparing field shock test data to draft shock design levels to ensure shock design criteria conservatively envelope actual field conditions, and (3) comparing the severity of shock pulses with different characteristics, including different shape, peak amplitude, jerk, and pulse duration. It is also referred to as a maximum response spectrum that can be used to analyze any dynamic event, even vibration signals [Reference C-7].

The SRS uses a model of the single-degree-of-freedom (SDOF) system shown in Figure C-1 to compute the effects of an input motion X (t) on the SDOF system. The system has a base attached to a mass (m) by a spring with stiffness k and a damper with damping coefficient c. For a prescribed time varying shock input motion X (t) at the base of the system the resulting response of the mass (m) is Y (t). The relative displacement Z (t) between the base and the mass is X (t) minus Y (t). The equation of motion of the system given by equation (C-1) is obtained by summing the inertial force of the mass and the forces within the spring and damper.

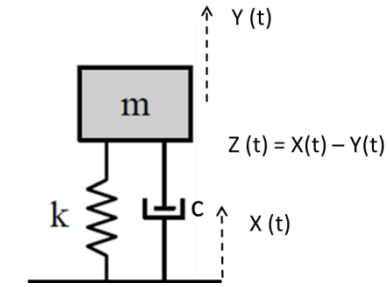

Figure C-1. Single-degree-of-freedom Mathematical Model

$$m\,\ddot{y}(t) = -k\,z(t) - c\,\dot{z}(t) \qquad \text{Equation (C-1)}$$

Where *t* is time and:

$$\xi = \frac{c}{2\,m\,\omega} \qquad \text{Equation (C-2)}$$

$$\omega = \sqrt{\frac{k}{m}} \qquad \text{Equation (C-3)}$$

The natural frequency (f) in Hertz (Hz) of the SDOF system is given by equation (C-4).

$$f = \frac{\omega}{2\pi} = \left(\frac{1}{2\pi}\right)\sqrt{\frac{k}{m}} \text{ Hz} \qquad \text{Equation (C-4)}$$

The solution of equation (C-1) provides the predicted response motion of the mass (m) caused by the base input motion either in terms of the absolute motion of the mass Y(t) or the relative motion Z(t) between the base and the mass.

An SRS is the maximum response of a set of single-degree-of-freedom (SDOF), spring-mass-damper oscillators to an input motion. The input motion is applied to the base of all oscillators, and the calculated maximum response of each oscillator versus the natural frequency make up the spectrum [C-7].

The relative displacement SRS is often used as a parameter to compare shock severity when two input shock motions are being compared. It is an intuitive engineering measure of severity because the relative displacement is proportional to the strain in the spring. The shock pulse that causes the larger strain, and therefore the largest damage potential, is judged to be the more severe of the two base input motions. Figure C2 shows three vertical acceleration time histories recorded at different locations on a planing craft. The plot on the right is the computed maximum relative displacement SRS (DSRS) for each time history. Visual inspection of the time histories on the left indicate that the red bow shock pulse is the most severe. The DSRS curves on the right quantify the difference in severity. The key feature of the SRS approach is that it quantifies shock severity based on its effect on a set of SDOF models.

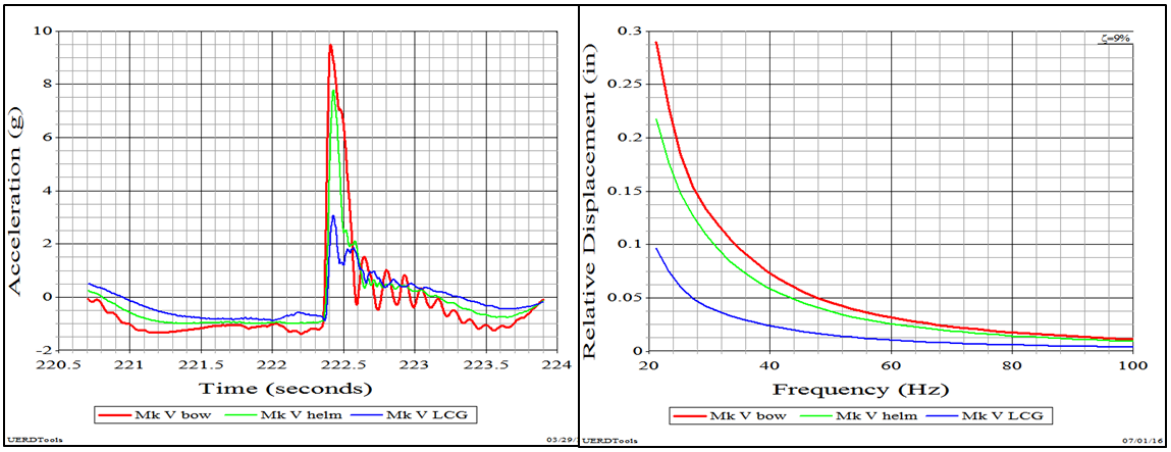

Figure C-2. Three Wave Slam Shocks and Relative Displacement SRS[5]

[5] All data plots and SRS shown in the report were created using UERDTools [C-8].

The following example illustrates use of DSRS to demonstrate that a shock pulse from a laboratory shock machine has equal or greater shock effects compared to a severe wave slam pulse. Figure C-3 shows two shock pulses. The red curve is a plot of vertical acceleration recorded during a severe wave impact at the bow of a craft. The shock portion of the time history has a peak of 8.5 g and pulse duration of 125 msec. The blue curve is the vertical shock pulse created by a laboratory shock machine during a test of the actual electronics enclosure. The shock machine was not capable of creating shock pulses with durations from 100 msec to 125 msec, but it could produce vertical pulses with 23-msec duration. The peak acceleration of the blue shock machine pulse is 10 g (i.e., 10 g – 23 msec half-sine pulse). The shock machine oscillations before and after the shock pulse are the run-up and after portion required to generate the 10 g half-sine pulse and return the table to its original position.

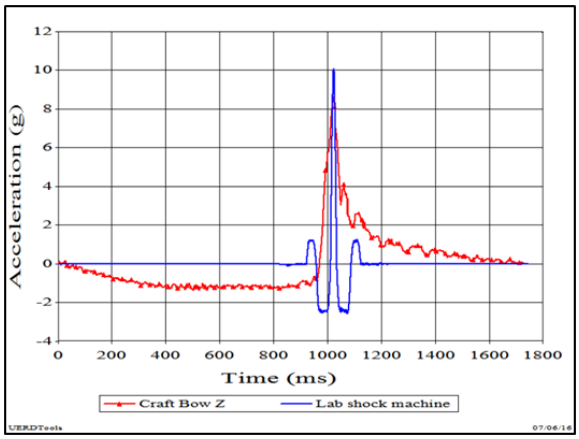

Figure C-3. Wave Slam and Shock Machine Pulses

Figure C-4 shows the DSRS computed using the two time history accelerations in Figure C-3 as shock inputs. The physical interpretation of the frequency scale in Figure C-4 is related to the natural frequencies of the fundamental modes of response of an equipment item (i.e., natural modes of vibration or eigenvalues). For SDOF natural frequencies greater than 10 Hz the DSRS for the shock machine pulse has a more severe effect (i.e., greater maximum relative displacements and greater strain in the springs) compared to the shock pulse of the actual wave impact. This indicates the machine test is more severe for SDOF systems with natural frequencies greater than 10 Hz. The machine test is therefore useful for mitigating the risk of failure at sea as long as the natural response modes of the electronics enclosure are greater than 10 Hz. Equipment natural frequencies are typically from 45-50 Hz to several hundred Hz.

The SRS can also be plotted using other SDOF response parameters as shown in Figure C-5. In this figure the spectra compare the severity of a 3g – 100-ms half-sine pulse to the severity of a 2 g – 150-ms half-sine pulse. The upper left plot shows the two input pulses in the time domain; the other three plots show maximum responses in the SRS frequency domain (i.e., as a function of oscillator natural frequency). The upper right plot shows how the absolute peak acceleration response of the mass varies with system natural frequency. They are called the absolute acceleration shock response spectra (ASRS).

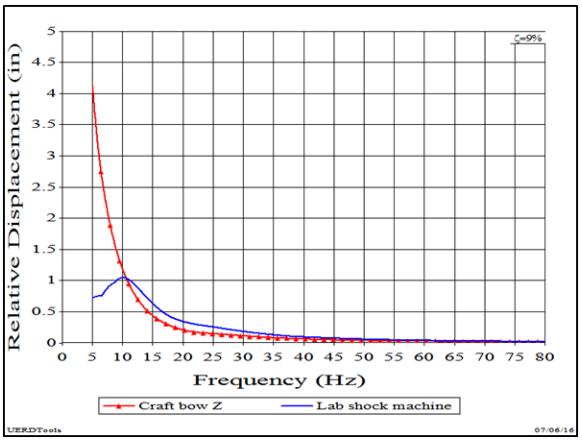

Figure C-4. DSRS for Wave Slam and Shock Machine Pulses

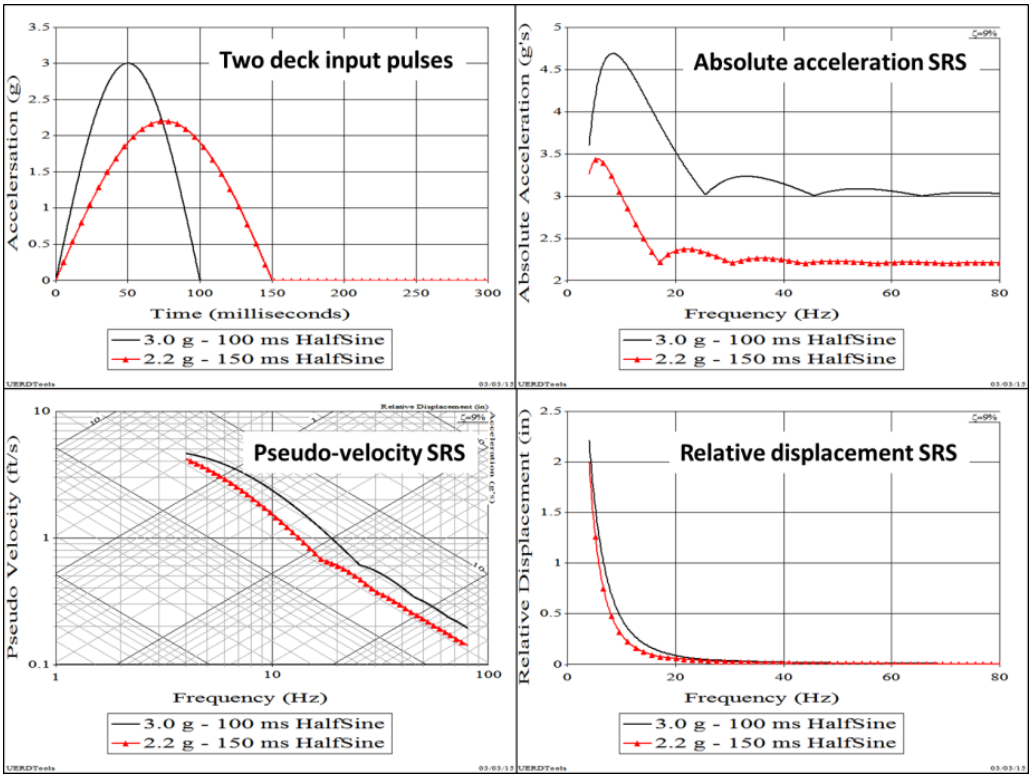

Figure C--5. Different Types of Shock Response Spectra

The lower right plot in Figure C-5 is the relative displacement SRS for each input pulse, and the lower left plot is the pseudo- velocity SRS (PVSRS) for each pulse. Logarithmic scales are used on all four axes of the PVSRS. The horizontal lines are the pseudo-velocity scale. Vertical lines are the system natural frequency scale. Lines sloping downward to the left show the predicted maximum relative displacement scales. Lines sloping downward to the right show the predicted maximum response accelerations. The log-log PVSRS is a useful format because it provides a measure of the shock severity in units of maximum relative displacement, velocity,

and acceleration. The acceleration scale is referred to as the pseudo-acceleration (A_{MAX}) for damped systems and the velocity scale is referred to as the pseudo-velocity when the maximum values are calculated using equations (C-5) and (C-6), which applies for lightly damped or zero damped systems [C-1]. Z_{MAX} is the maximum relative displacement.

$$A_{MAX} = (2\pi f)^2 Z_{MAX} \qquad \text{Equation (C-5)}$$

$$V_{MAX} = (2\omega f) Z_{MAX} \qquad \text{Equation (C-6)}$$

Appendix C References

C-1. Harris, Cecil M., editor-in-chief, *Shock and Vibration Handbook, Fourth Edition*, McGraw-Hill Companies, Inc., New York, New York, 1995.

C-2. ANSI/ASA S2.62-2009, *Shock Test Requirements for Equipment in a Rugged Shock Environment*, American National Standards Institute and Acoustical Society of America, Melville, N.Y., 2009.

C-3. Department of Defense Test Method Standard, *Environmental Engineering Considerations and Laboratory Tests*, Military Standard, MIL-S-810G, change 1, Method 516.7, Shock, 15 April 2014.

C-4. STANAG 4559, *Testing of Surface Ship Equipment on Shock Testing Machines*, NATO Standardized Agreement, 13 May 2008.

C-5. Alexander, J. Edward, *The Shock Response Spectrum – A Primer*, Society of Experimental Mechanics Inc., Proceedings of the IMAC XXVII, Orlando, Florida, USA, 9 – 12 February 2009.

C-6. Gaberson, Howard A., *Shock Severity Estimation*, Sound and Vibration Magazine, Volume 46 Number 1, January 2012.

C-7. ISO-18431-4: 2007, *Mechanical vibration and shock – Signal processing – Part 4: Shock response spectrum analysis*, International Organization for Standardization, Geneva, Switzerland, 2007.

C-8. Mantz, Paul A., Costanzo, Fredrick A., *An Overview of UERDTools Capabilities: A Multi-Purpose Data Analysis Package*, Proceedings of the IMAC-XXVII Conference and Exposition on Structural Dynamics, Society of Experimental Mechanics, Inc., 9-12 February 2009, Orlando, Florida, 2009.

THIS PAGE INTENTIONALLY LEFT BLANK

Appendix D. Shock Isolation

Shock Isolation Theory

The following examples apply to passive spring-damper assemblies with no feedback mechanism (active or semi-active) to control the input or response of a shock isolation system. Many, but not all, of these passive isolation systems exhibit linear stiffness and damping curves over a range of relative motion across their spring-damper assemblies. The linear single-degree-of-freedom (SDOF) model shown in Figure D-1 is therefore a useful model for understanding concepts of shock isolation. Systems with non-linear characteristics can be studied using finite difference solution approaches that are beyond the scope of this appendix. In theory the mass shown in Figure D-1 can represent a fragile equipment item to be protected by shock mounts or it could represent the combined weight of a seat and its occupant secured to the seat with a seat belt.

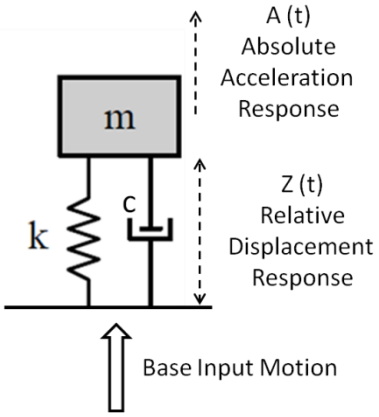

Figure D-1. SDOF Model of Spring-damper Shock Isolation System

The natural frequency (f) in Hertz (Hz) of the spring-mass assembly is given by equation (D-1), where (m) is the mass and (k) is the stiffness of the spring. The damping coefficient is (c).

$$f = \frac{\omega}{2\pi} = \left(\frac{1}{2\pi}\right)\sqrt{\frac{k}{m}} \text{ Hz} \qquad \text{Equation (D-1)}$$

Example calculations will be shown for two different shock isolation systems for an assumed base input acceleration of 7 g – 100 msec (half-sine shape). One isolation mount is a

10-Hz system with 20% damping, and the other is a 2-Hz system with 20% damping. Figure D-2 shows the half-sine input acceleration (i.e., black curve) and the calculated responses for the two isolators. The plots clearly show that the 10-Hz isolator (red curve, circle symbols) with a peak response acceleration of 9.5 g amplifies the input by about 35 percent (9.5/7 = 1.35) while the 2 Hz system (blue curve, triangle symbols) with a peak response of 4.1 g mitigates the input about 42 percent (1-4.1/7=0.42). This shows in a time history format that if the isolator frequency is not chosen properly the isolation system will not mitigate the 7 g wave slam pulse.

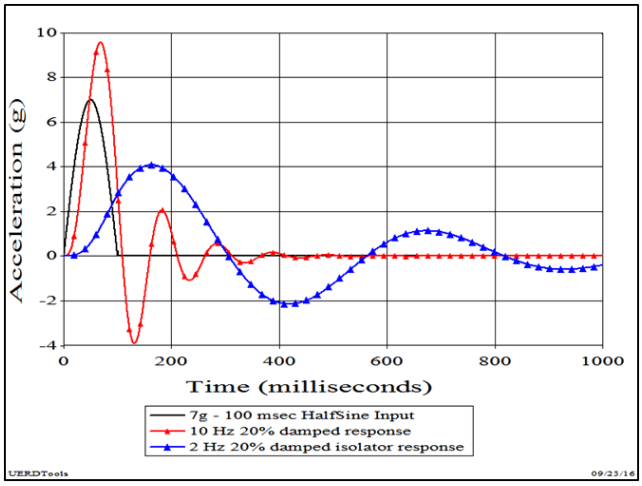

Figure D-2. Base Input and Shock Isolator Responses

The same results can be shown using a maximum acceleration SRS for the 7 g input pulse (assuming 20% damping) as shown in Figure D-3. The plot is the maximum absolute acceleration response of the mass as a function of system natural frequency. At 2 Hz the ASRS value is 4.1 g (triangle symbol), and at 10 Hz the ASRS is 9.5 g (circle symbol), the same as the peak accelerations shown in Figure D-2.

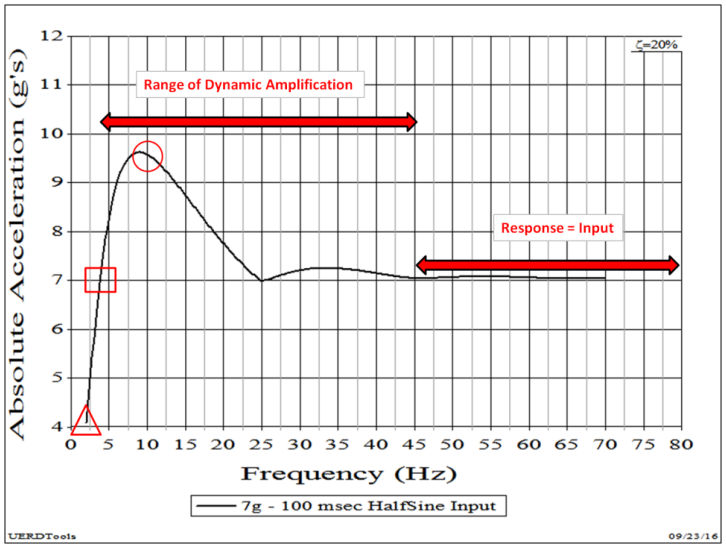

Figure D-3. ASRS of the 7 g – 100 msec Input Pulse

The square symbol in Figure D-3 corresponds to the frequency limit value where the mass's peak acceleration response is equal to the input (i.e., 7 g). Shock mitigation only occurs for natural frequencies below this limit value. The limit value and the percent of mitigation depend upon the isolator damping. In this example the limit value is approximately 3.1 Hz. Isolation systems with natural frequencies below 3.1 Hz will mitigate the shock input if sufficient excursion space is allowed to prevent mount bottoming. Isolation systems with natural frequencies from 3.1 Hz to about 45 Hz amplify the base input motion (i.e., dynamic amplification). Above 45 Hz the isolator acts like a rigid link and merely transmits the base input acceleration.

The calculations shown in Figures D-2 and D-3 apply only to the 7 g base input acceleration and 20% damping ratio. It is possible however to combine information from many ASRS plots for different amplitude inputs and damping values in the non-dimensional format shown in Figure D-5. It has the same shape as the ASRS in Figure D-3, but the ordinate axis is the mitigation ratio (MR = response DSRS/input DSRS) and the abscissa is the value R[6]. R is the ratio of half-sine pulse duration (in seconds) divided by the natural period of the isolation system given by equation (D-2), or the product of the half-sine pulse duration (in seconds) and the natural frequency of the isolation system.

$$R = \frac{T}{\tau} = T\left(f_{SYS}\right) \qquad \text{Equation (D-2)}$$

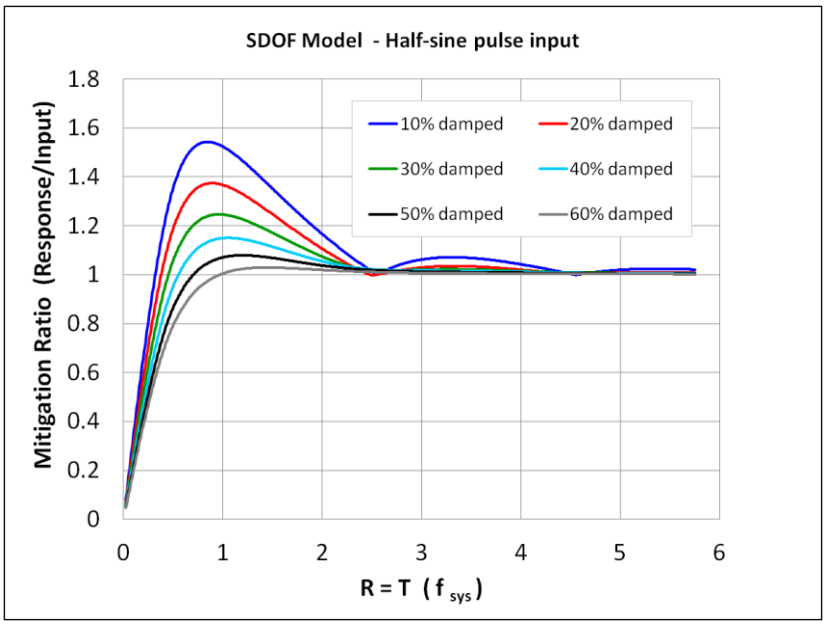

Figure D-5. Shock Mitigation Ratio for Half-sine Pulse

[6]Some references use the half-sine period (2T) rather than the half-sine pulse duration (T).

In Figure D-5 the limit values of R are where the MR (mitigation ratio) curves cross over from amplification to mitigation at MR = 1.0 for different damping ratio values. For example, the blue curve for 10% damping crosses a mitigation ratio of 1.0 when the R value is 0.314. Thus mitigation is achieved for a mount with 10-percent damping only when R is less than 0.314 (i.e., the limit value for 10% damping). As damping increases from 20 percent to 60 percent the curves show that the R limit value moves to the right: 0.382 for 20%, 0.455 for 30%, 0.557 for 40%, 0.704 for 50%, and 0.971 for 60%. These curves apply for any below mount peak half-sine pulse acceleration amplitude because the SDOF system was assumed to be a linear model. For example, if the below mount input is 7 g – 100 msec, the above mount peak acceleration will also be 7 g when R = 0.314.

An example of shock mounts that amplify wave slam shock inputs is illustrated in Figure D-6. The upper acceleration data plot shows the vertical acceleration input recorded below the shock isolation mounts (blue curve). The vertical acceleration response above the mounts at the equipment item is the red curve. The pulse durations of the blue input and red response curves are approximately the same, but the peak accelerations above the mounts are greater than below the mounts. The explaination for this amplification can be shown mathematically using the single degree of freedom (SDOF) model shown in the figure. The black curve in the lower right plot is the same acceleration below the mounts shown in the upper plot between 348 and 349 seconds. It was used as the shock input pulse for the SDOF model. The red curve in the lower right plot is the predicted motion above the mounts for a shock isolation system with a natural frequency of 12 Hz and 20% damping. The time-history prediction shows shock mount amplification response similar to that observed in the data.

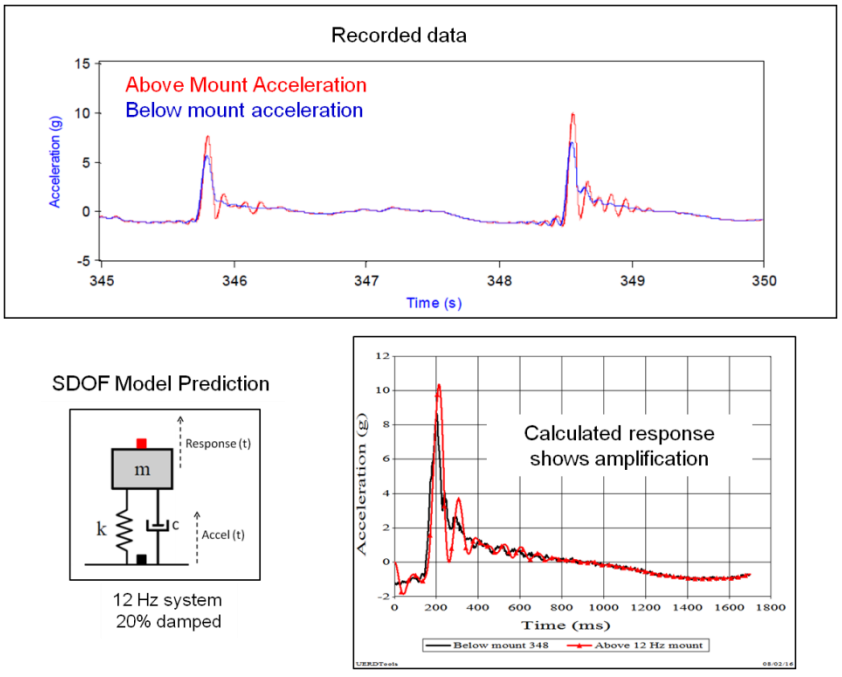

Figure D-6. Recorded and Predicted Shock Mount Amplification

In Figure D-6 the shock pulse duration for the wave slam recorded between 348 and 349 seconds is approximately 0.15 seconds. For a 12-Hz mount this corresponds to an R value of 1.8. Figure D-5 shows that R = 1.8 for 20% damping is in the shock amplification region with a predicted mitigation ratio of approximately 1.18. For 20% damping shock mitigation requires an R value less than approximately 0.38 (i.e., the limit value for 20% damping). Selection of new mounts for this installation would focus on MR values less than the R limit value while ensuring that sufficient excursion space is allowed to prevent mount bottoming.

THIS PAGE INTENTIONALLY LEFT BLANK

Distribution

	Hard Copies	*Digital Copies*
Naval Sea Systems Command PEO Ships, PMS 325G 1333 Isaac Hull Ave, SE Building 197 Washington Navy Yard, DC 20376 Attn: Christian Rozicer		1
Naval Sea Systems Command TWH Small Boats and Craft 2600 Tarawa Court, Suite 303 Virginia Beach, VA 23459 Attn: Mr. Dean Schleicher		1
Commander Office of Naval Research Sea Platforms and Weapons Division 875 North Randolph Street, Arlington, VA 22203-1995 Attn: Dr. Robert Brizzolara, Code 333		1
Commander U. S. Special Operations Command 7701 Tampa Point Boulevard MacDill Air Force Base, FL 33621-5323, Attn: W. Boudreaux, SORDAC-M-SS		1
Commander Naval Special Warfare Dev Group 1639 Regulus Avenue Virginia Beach, VA 23461-2299 Attn: Brian Pierce, Code N54-4		1
United States Naval Academy Hydromechanics Lab 590 Holloway Road Annapolis, MD 21402 Attn: John Zseleczky		1
United States Coast Guard RDT&E Division 2100 Second Street, SW STOP 7111 Washington, DC 20593-7111 Attn: W. Lew Thomas		1
Defense Technical Information Center 8725 John J. Kingman Road Fort Belvoir, VA 22060-6218		1

NSWC, CARDEROCK DIVISION INTERNAL DISTRIBUTION

Code	Name	*Hard Copies*	*Digital Copies*
661	Rhonda Ingler		1
809	Donna Intolubbe		1
836	Technical Data Repository		1
830X	Dr. Timothy Coats		1
831	Willard Sokol, III		1
832	Scott Petersen		1
833	Kent Beachy		1
833	Dr. Evan Lee		1
835	David Pogorzelski		1
835	Kelly Haupt		1
835	Heidi Murphy		1
835	Brock Aron		1
835	Jason Bautista		1
835	John Barber		1
1033	TIC-SCRIBE		1

NSWC PANAMA CITY

Code	Name	*Hard Copies*	*Digital Copies*
E41	Eric Pierce		1
E23	Brian Price		1
E41	Jeff Blankenship		1


NAVSEA
WARFARE CENTERS
Carderock